

Review

Neutral Metal 1,2-Dithiolenes: Preparations, Properties and Possible Applications of Unsymmetrical in Comparison to the Symmetrical

George C. Papavassiliou ^{1,*}, George C. Anyfantis ² and George A. Mousdis ¹

¹ Theoretical and Physical Chemistry Institute, National Hellenic Research Foundation, 48, Vassileos Constantinou Ave., Athens 11635, Greece; E-Mail: gmousdis@eie.gr

² Center for Biomolecular Nanotechnologies, Italian Institute of Technology (IIT), Via Barsanti, Arnesano, (LE) Lecce 73010, Italy; E-Mail: georgios.anyfantis@iit.it

* Author to whom correspondence should be addressed; E-Mail: pseria@eie.gr; Tel.: +30-210-7273-827; Fax: +30-210-7273-794.

Received: 19 March 2012; in revised form: 28 May 2012 / Accepted: 31 May 2012 /

Published: 29 June 2012

Abstract: This paper is an overview concerning the preparations and properties as well as possible applications of neutral (one component) metal 1,2-dithiolenes (and selenium analogues). The structural, chemical, electrochemical, optical and electrical behavior of these complexes depend strongly on the nature of ligand and/or the metal. The results of unsymmetrical in comparison to those of symmetrical complexes related to the properties of materials in the solid state are primarily discussed. The optical absorption spectra exhibit strong bands in the near IR spectral region *ca.* 700 to *ca.* 1950 nm. X-ray crystal structure solutions show that the complexes usually have square-planar geometry with S–S and/or M–S contacts. Some of them behave as semiconductors or conductors (metals) and are stable in air. The cyclic voltammograms at negative potentials are different from the corresponding potentials of tetrathiafulvalenes (TTFs). As a consequence, the LUMO bands occur at much lower levels than those of TTFs. Consequently, electrical measurements under conditions of field effect transistors exhibit n-type or ambipolar behavior. Illumination of materials with high power lasers exhibits non-linear optical behavior. These properties enable metal 1,2-dithiolene complexes to be classified as promising candidates for optical and electronic applications, (e.g., saturable absorbers, ambipolar inverters).

Keywords: neutral metal 1,2-dithiolenes; semiconductors; field effect transistors; optical properties; nonlinear optical properties

1. Introduction

During the last five decades, a number of regular papers, review articles and chapters in books, concerning the synthesis and properties of metal 1,2-dithiolene (M 1,2-DT) complexes and selenium analogues, with $M = \text{Ni}, \text{Pd}, \text{Pt}, \text{Au}, \text{Cu}$, *etc.*, have been published (see for example [1–114]). The (neutral) complexes are characterized as homoleptic with the general formula (Figure 1) or heteroleptic such as M(diimine)(dithiolate). The homoleptic are divided in symmetrical with $R_1 = R_2 = R_3 = R_4$ (R-family, not cyclic), with $R_1, R_2 = R_3, R_4$ (RR-family, cyclic), with $R_1 = R_2 = R_3 = R_4 = \text{SR}$ (SR-family, not cyclic), with $R_1, R_2 = R_3, R_4 = \text{S-R-S}$ (SRS-family, cyclic), with $R_1, R_2 = R_3, R_4 = \text{N(R)-C(=S)-N(R')}$ (NNR-family, cyclic), *etc.*, as well as unsymmetrical with $R_1 = R_2 \neq R_3 = R_4$ (R-family, not cyclic), with $R_1, R_2 = \text{RR} \neq R_3, R_4 = \text{R'R'}$ (R'R'-family, cyclic), with $R_1, R_2 = \text{S-R-S} \neq R_3, R_4 = \text{S-R'-S}$ (SR'S-family, cyclic), *etc.* Some of the simple ligands and their abbreviations are tabulated in Table 1. Some ligands with complicated edge groups are referred by numbers and tabulated in Table 2 (see also [10,97]). The additional groups to the metal dithiolene core could have donor ability (e.g., OMe, NMe₂) or acceptor ability (e.g., CN, CF₃). The donor (push) or acceptor (pull) ability of the additional groups, plays an important role in the behavior concerning optical, conducting and superconducting properties of these materials. For example, the complexes [M(mnt)₂] [5] and [M(dmit)₂] [6] (see also [8,11,12,20]), of which the molecular formulas are shown in Figure 2, are based on the ligands with acceptor groups and give cation deficient salts. Since the observation of semiconducting behavior in (Li)_x[Pt(mnt)₂] [5] and (Bu₄N)_x[Ni(dmit)₂] ($1 > x > 0$) ([6] and references therein), a number of similar complexes based on Ni, Pt, Pd, Cu and Au have been prepared and studied.

Figure 1. General molecular formula of neutral M 1,2-DT complexes.

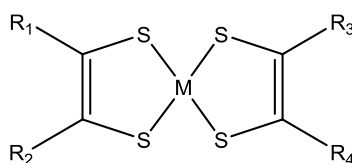


Figure 2. Molecular formulas of Ni(mnt)₂ and Ni(dmit)₂.

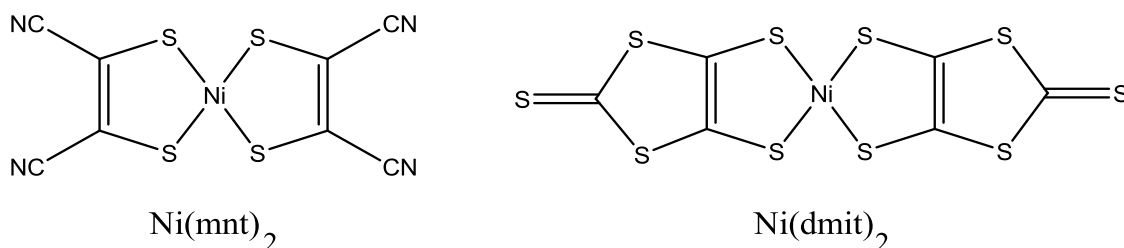


Table 1. Simple 1,2-dithiolene ligands and their abbreviations.

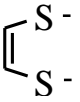
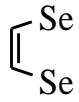
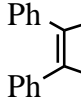
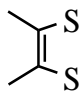
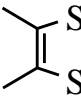
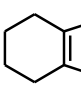
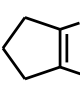
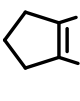
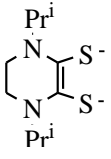
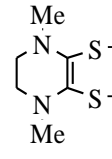
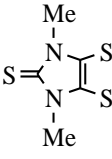
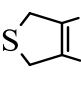
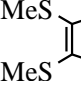
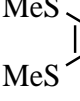
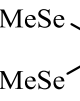
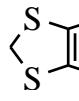
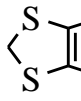
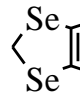
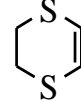
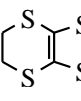
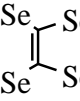
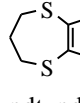
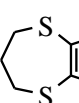
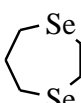
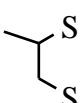
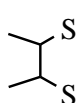
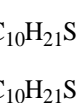
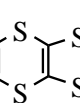
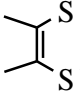
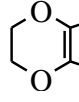
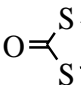
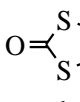
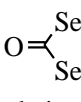
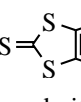
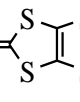
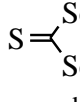
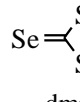
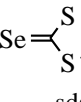
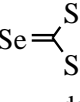
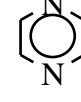
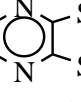
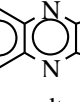
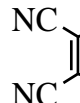
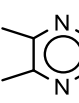
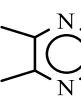
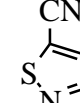
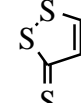
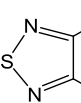
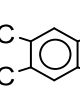
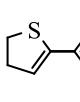
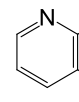
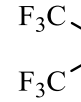
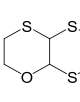
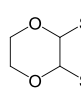
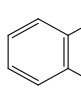
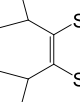
						
edt	eds	dpedt	dmedt	dmeds	temedt	tmedt
						
tmeds	Pr ⁱ ₂ pipdt	Me ₂ pipdt	Me ₂ timdt	tdmdt	mtdt, dtm	mtds
						
bmsds	mdt	mds	msds	dddt	ddds	dsdds
						
pdt, pddt, dddt	pds, pdds	psdds	mddd	dmddd	dcddt	dddt
						
dmvd	edo	dmio, dmid	dtods	dmios, dsods	dmit	sdsit
						
dsit	dmis(e)	sdsit	dsis	prdt	prds	qdt
						
mnt	dmprdt	dmprds	dcit	i-dmit	tdqs, tds	dcdbt
						
tbd	pydt	hfdt	etodddt	edodddt	bdt	dipht

Table 2. Some 1,2-dithiolene ligands referred by numbers.

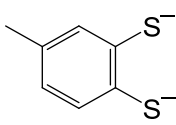
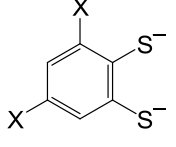
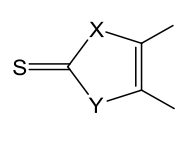
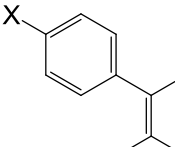
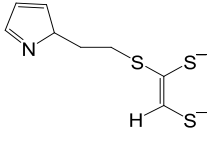
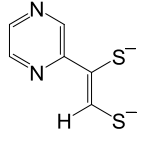
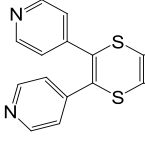
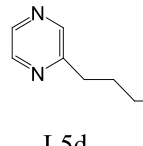
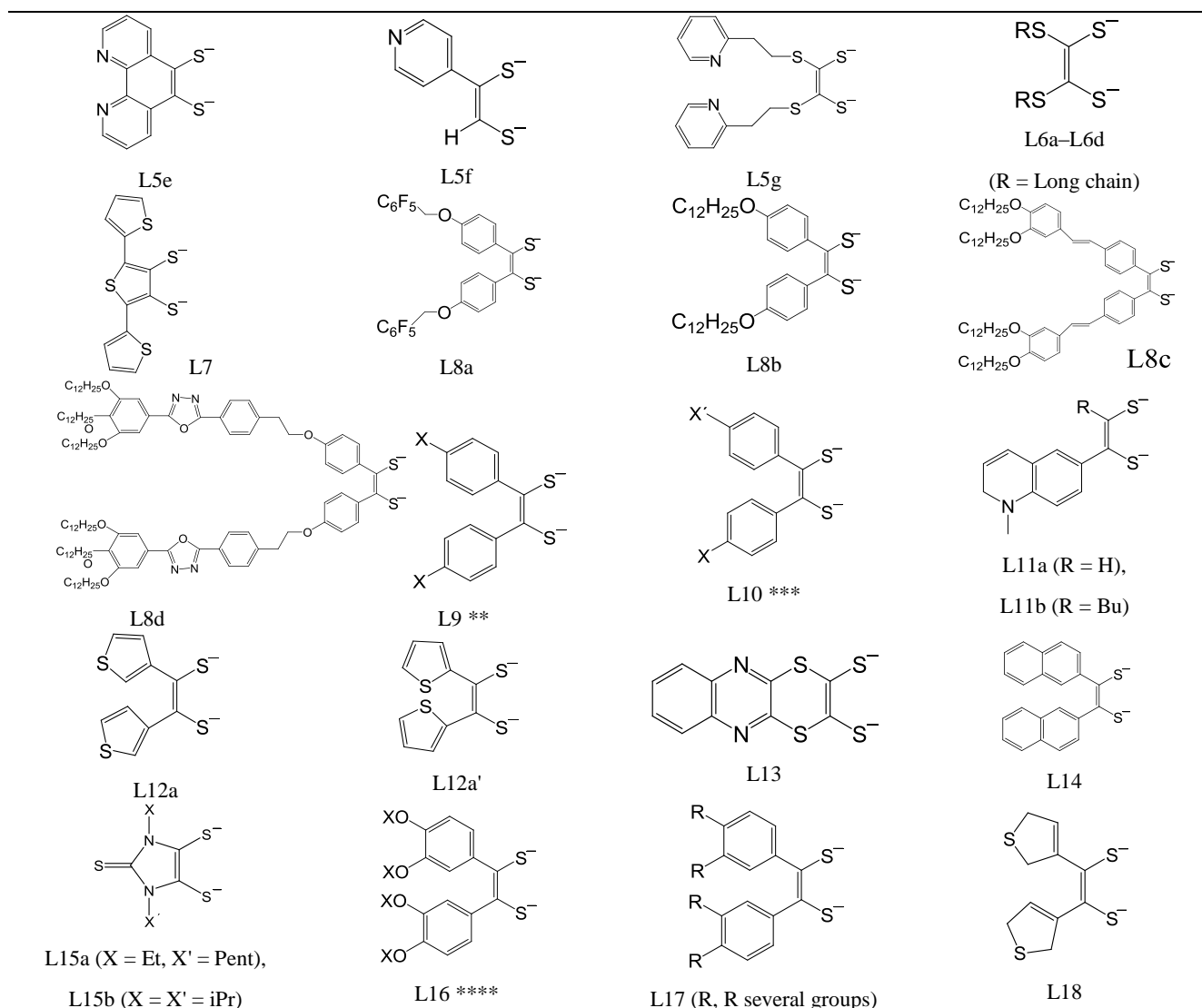
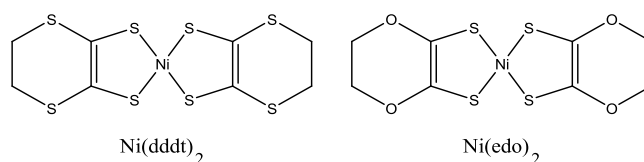
			
L1	L2a (X = Br)	L3a (X = S, Y = NR)	L4*
			
L5a	L5b	L5c	L5d

Table 2. Cont.



* L4a (X = Me), L4b (X = Br), L4c (X = F), L4d (X = CF₃), L4e (X = NO₂), L4f (X = Cl), L4g (X = CN), L4h (X = H), L4i (X = OMe); ** L9a (X = H), L9b (X = Me), L9c (X = Et), L9d (X = F), L9e (X = CF₃), L9f (X = tBu), L9g (X = C₆H₆), L9h (X = COOH), L9i (X = COOMe), L9j (X = OMe), L9k (X = OC₄H₉), L9l (X = OC₈H₁₇), L9m (X = OC₁₂H₂₅), L9n (X = OC₁₄H₂₉), L9o (X = OC₁₆H₃₃), L9p (X = OC₁₈H₃₇); *** L10a (X = H, X' = NMe₂), L10b (X = OMe, X' = OH), L10c (X = Oethylexyl, X' = OH), L10d (X = OC₁₀H₂₁, X' = OH), L10e (X = OC₁₀H₂₁, X' = OMe), L10f (X, X' = Several groups); **** L16a (X = H), L16b (X = Me), L16c (X = C₁₂H₂₅).

On the other hand, the complexes [Ni(dddt)₂] [5] and [Ni(edo)₂] [14], of which the molecular formulas are shown in Figure 3, are based on ligands with donor ability and give cationic salts, which are conducting materials [13–15,21].

Figure 3. Molecular formulas of Ni(dddt)₂ and Ni(edo)₂.

The M 1,2-DT complexes exhibit some similarities to the so called TTF compounds of the general formula (Figure 4) and selenium analogues, in which the central metal atom (M) of M 1,2-DTs is replaced by the C=C group (see for example [12,16,21,85]). Generally, the TTFs such as ET (Figure 5), exhibit weak semiconducting behaviour with energy gap of 2–3 eV, while M 1,2-DTs are better semiconductors with HOMO/LUMO energy gap smaller than 1.5 eV. Some cationic salts of TTFs exhibit similar behavior to that of M 1,2-DT cationic salts. For example $[\text{Ni}(\text{ddd})_2]_2\text{X}$ are isostructural and exhibit metallic behavior as $(\text{ET})_2\text{X}$.

Figure 4. General molecular formula of TTF compounds.

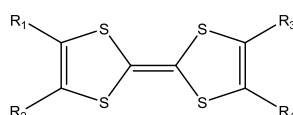
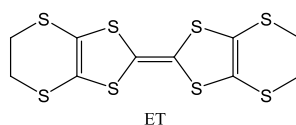


Figure 5. Molecular formula of ET.



In recent years, a number of symmetrical M 1,2-DT complexes based on extended TTF-dithiolato ligands, such as $[\text{Ni}(\text{dt})_2]$ [22,23] and some unsymmetrical such as $[\text{Ni}(\text{dt})(\text{dmit})]$ [48,49] (Figure 6) and selenium analogues have been prepared and studied. A number of extended TTF-dithiolate ligands are tabulated in Table 3. Dithiolene ligands could be coordinated as 1,2-enedithiolate dianions (as in Tables 1–3), neutral dithioketones or mixed valence thioketones—radical thiolate monoanions—and have been regarded both as innocent and non-innocent ligands [6–10,49,68]. These single component (neutral) complexes exhibit semiconducting or metallic behaviour. Review articles, concerning neutral complexes with N coordinated groups [97] or with ligands of Table 2 [102] and articles concerning unsymmetrical complexes (of the type push-pull) [95], have been reported recently.

Figure 6. Molecular formulas of $\text{Ni}(\text{dt})_2$ and $\text{Ni}(\text{dt})(\text{dmit})$.

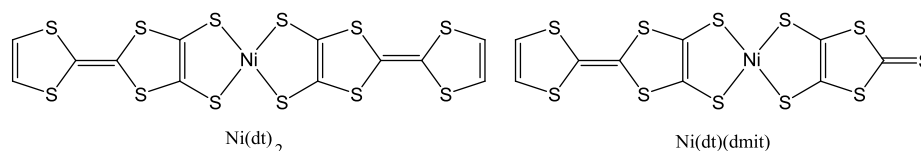
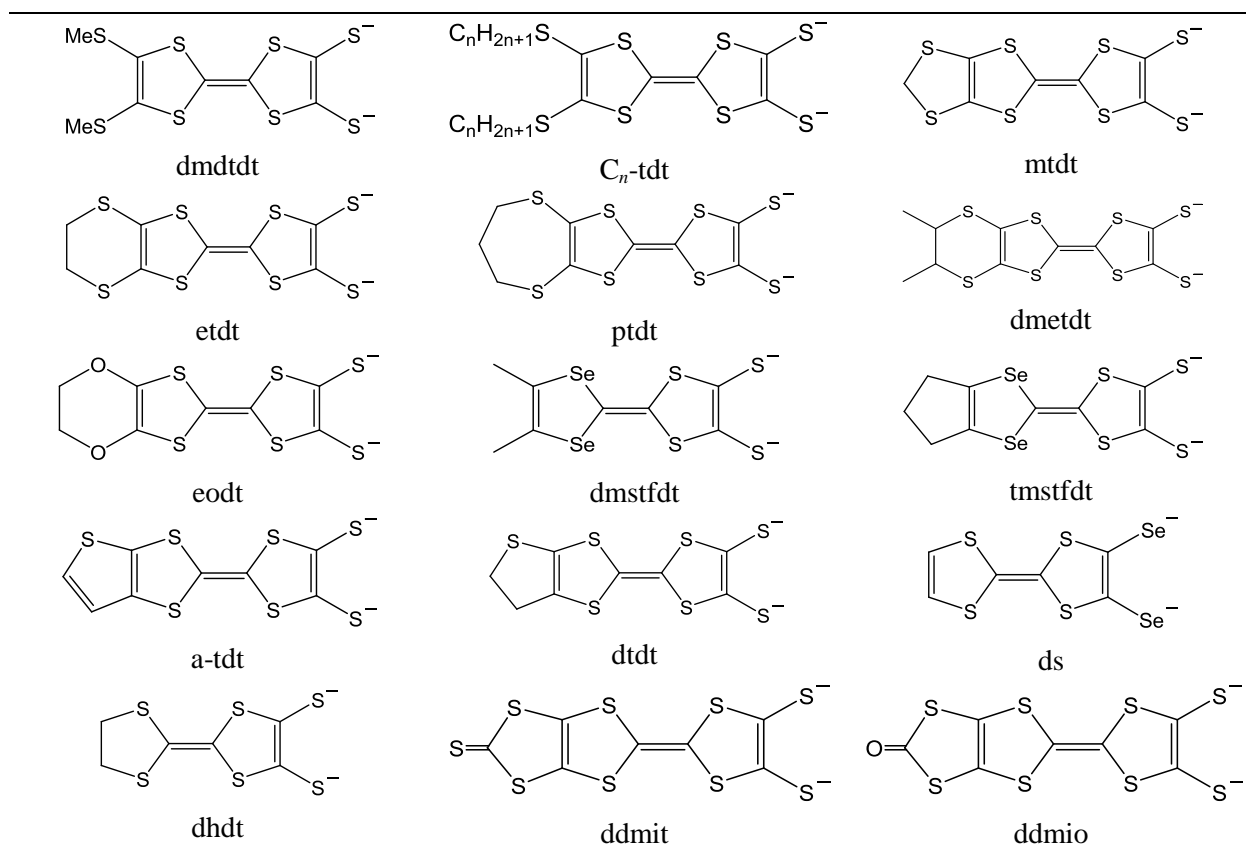


Table 3. Extended TTF 1,2-dithiolene ligands and their abbreviations.

dt	dmdt	tmdt
dpdt	chdt	hfdt

Table 3. Cont.



This paper is an overview of the published work concerning the preparation, properties and possible applications of semiconducting neutral (single component) complexes based on Ni, Pt, Pd, Cu, Au and on some ligands of Tables 1–3. Mainly, the work published since 2005 is considered [1–114]. The results, obtained from unsymmetrical complexes in comparison to the corresponding symmetrical ones in the solid state, are mainly discussed. They are compared to those obtained from the corresponding TTFs and similar single component materials. More information concerning the ligands of Table 1 can be found in [6–16,20,21,24,26–28,30,31,34,36,48–50,53,61–64,72,77,79,88,89,92,94,100–104]. More information concerning the ligands of Table 2 can be found in the corresponding references for L1 [34], L2 [34,98], L3 [33,95,102], L4 [56,73,102], L5 [97], L6 [61], L7 [75], L8 [58,60], L9 [56,60,79,84,101,110,111], L10 [38,62,65,79,101,102,110], L11 [109,113], L12 [93,102], L13 [114], L15 [33,102,114], L16 [57,102], L17 [102], and L18 [93,102]. More information concerning the ligands of Table 3 can be found in the references [22,23,30,45,46,48,49,90]. Some related papers are given in references [115–139]. They concern properties of TTFs [117,130–133], structural [115,123], and electronic [118–121] properties of solids, electrochemical aspects [122], saturable absorbers [121] and field effect transistors [116,124–129,134–138].

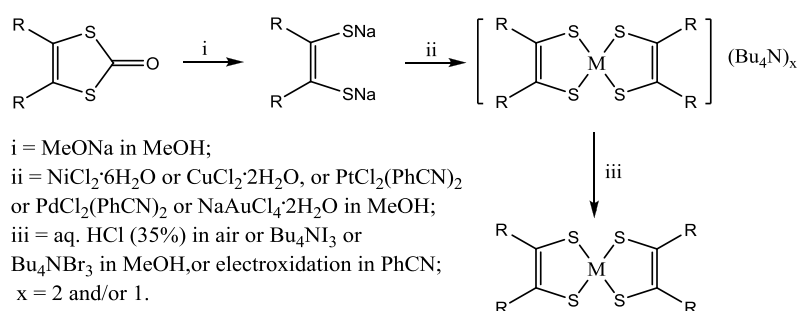
2. Experimental Methods/Techniques

2.1. Preparations

The first metal 1,2-dithiolene, the neutral bis[1,2-diphenyl-1,2-ethylenedithiolato (2⁻)-kS₁,kS₂] nickel, abbreviated as [Ni(dpdt)₂], was reported in 1962, derived from the reaction of diphenylacetylene

with nickel sulfide [1]. Since then this compound and the Pt and Pd analogues have been prepared by reaction of benzoin with P_4S_{10} , followed by addition of $NiCl_2$, K_2PtCl_4 , and K_2PdCl_4 , respectively [2]. Today, a number of alternate methods are known, some of which are outlined here. The choice of method depends, amongst other things, on the availability of the starting materials. Usually, as in the case of the preparation of TTFs [9,12,16], 1,3-dithiole-2-ones have been used as starting materials [12,16,70,73–75,97,113] and the required neutral M 1,2-DTs were obtained from them, according to a three-step procedure of Scheme 1.

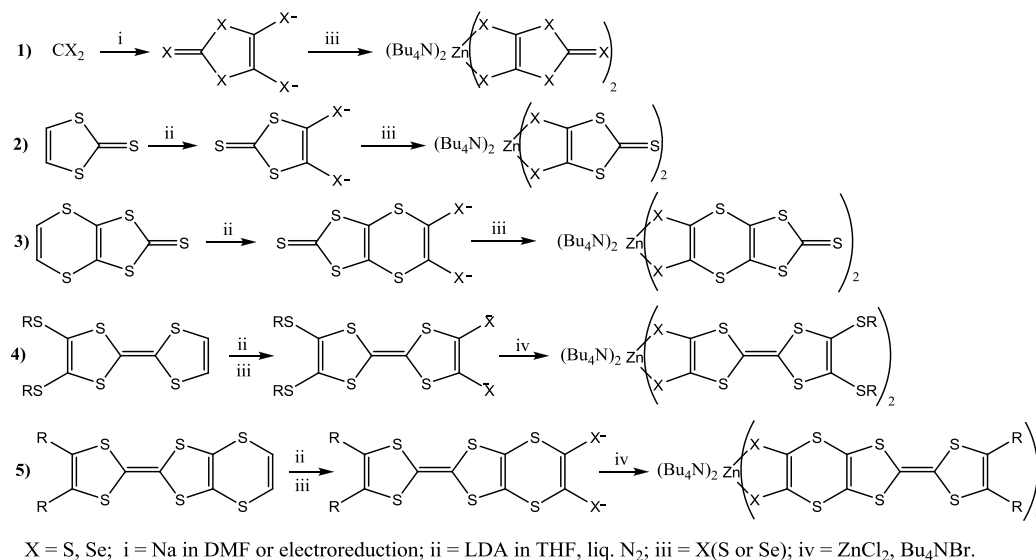
Scheme 1. Procedure for synthesis of M 1,2-DTs from 2-ketones.



It should be noted that the choice of the oxidizing reagent (iii) or the electrooxidation conditions to obtain the neutral compounds is based on redox potentials of the corresponding anionic complexes (see below section 5).

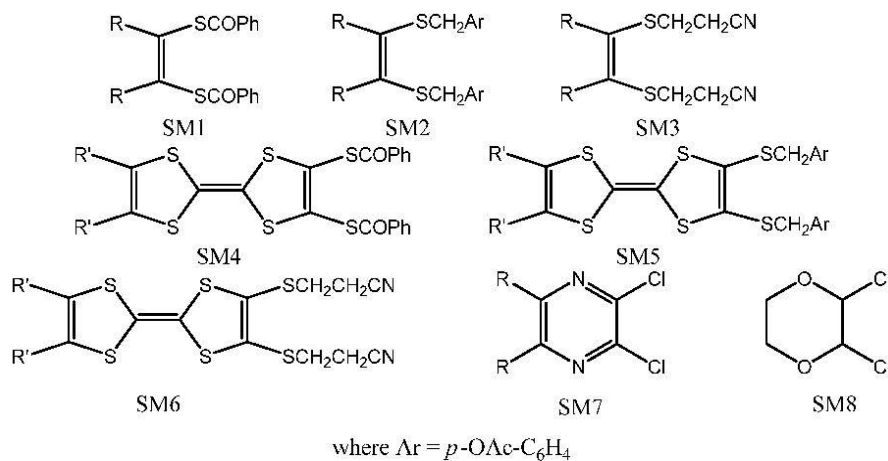
With this method, the neutral complexes $[Au(dpdt)_2]$ [79] and $Cu(L11)_2$ [109] have been prepared, recently. In most cases, the deprotection of the ligand precursor is made with MeONa in N_2 atmosphere and the addition of $NiCl_2$ at low temperature [22]. In some cases, e.g., when the ligand is dmit, dmio and etdt, cation deficient ($1 > x > 0$) complexes are obtained, instead of neutral ones (see [6,12]). Also, the anionic salts, precursors of neutral complexes, could be obtained from several starting materials (e.g., CS_2 , CSe_2 , vinylene trithiocarbonate) through the dianionic complexes of Zn or Hg (see [6,9,12,16,30,130,131] and references therein) as in the procedures of Scheme 2.

Scheme 2. Procedures for syntheses of M 1,2-DTs from several starting materials.



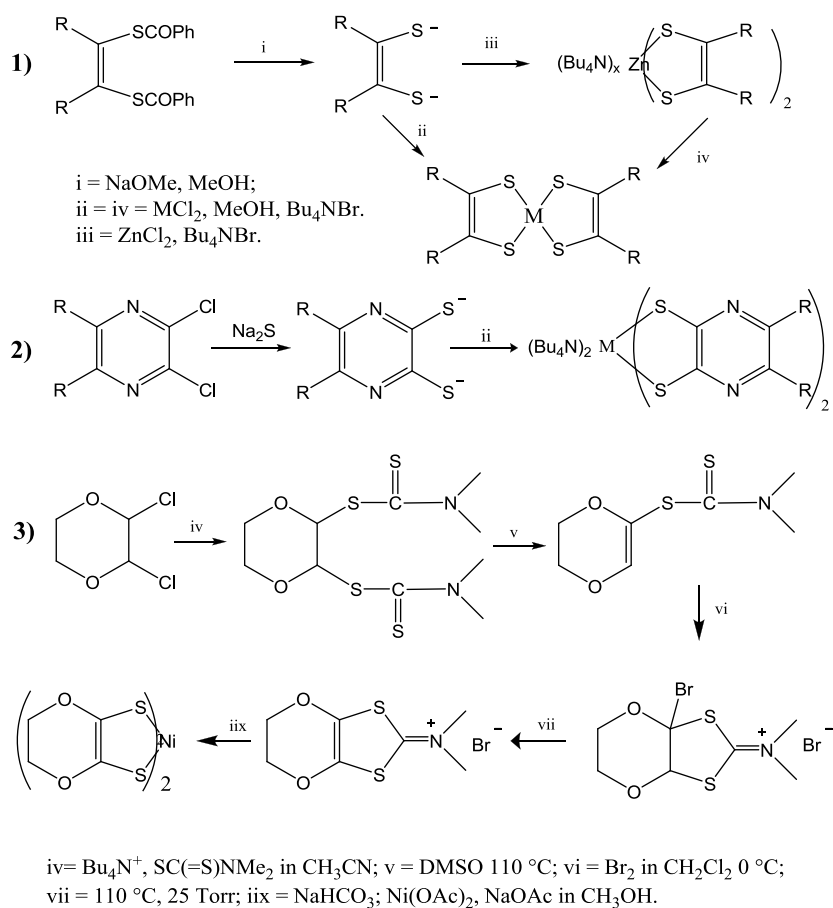
These Zn (or Hg) based anionic complexes react with NiCl_2 , $\text{PtCl}_2(\text{PhCN})_2$, *etc.* to give the corresponding mono and/or dianionic complexes of Ni, Pt, *etc.* [9,12,16]. Also, using the compounds of Figure 7 and selenium analogues, as starting materials, the preparation of (neutral) M 1,2-DTs is possible (see [9,14,36,48–50,52,63,64]).

Figure 7. Molecular formulas of a variety of starting materials.



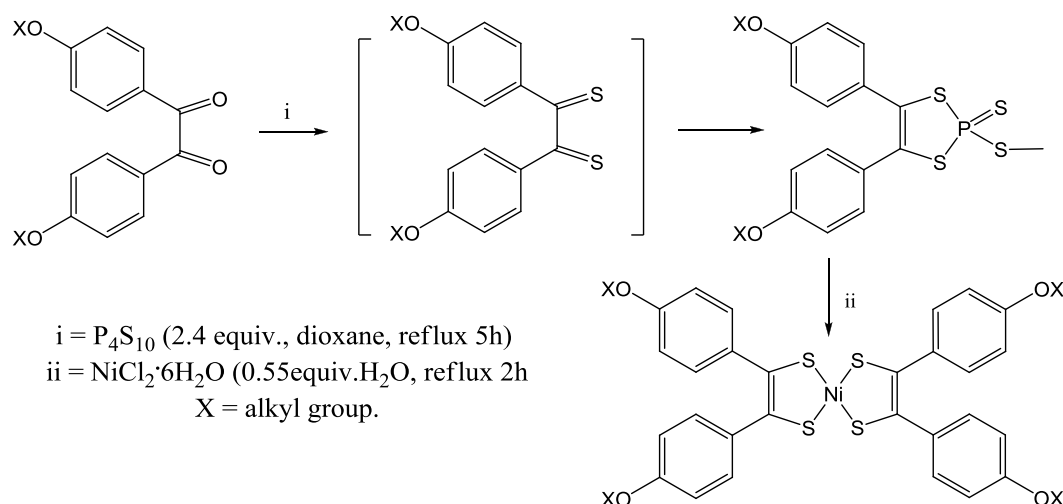
Some examples of reactions are given here, in Scheme 3 [9,16,52].

Scheme 3. Some examples of reactions, using starting materials of Figure 7.



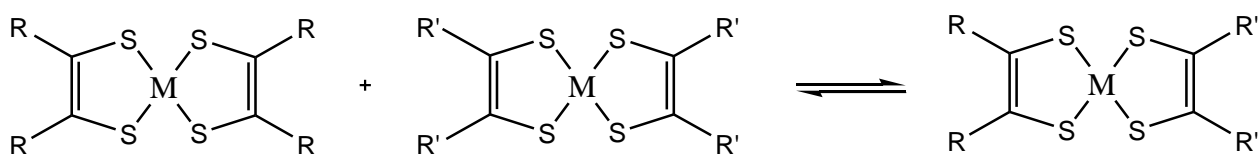
The old method, using 1,2-diketones (or benzoin)s as starting materials, was applied for the preparation of a number of neutral complexes. The first step of the reactions is the conversion of diones to dithions and/or to the phosphorus thioesters with P_4S_{10} or Lawesson's reagent. The next step of the reactions is the hydrolysis and then the formation of neutral complexes using metal carbonyl or other reactive salts, e.g., $NiCl_2$, $PdCl_2(PhCN)_2$. The following Scheme 4 gives an example of the preparation of a series of complexes from the corresponding 1,2-diketones [44,60,65,68,89,98,101,110,111].

Scheme 4. Procedure for preparation of M 1,2-DTs from 1,2-diketones.

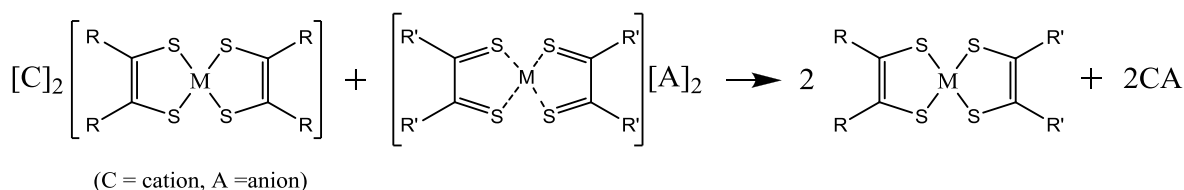


The unsymmetrical neutral complexes could be prepared by a ligand exchange reaction, which is affected by refluxing two different neutral complexes as in the (reversible) reaction of Scheme 5 (see [4,14]), or by refluxing a neutral and a dianionic or two equivalent monoanionic complexes, followed by oxidation. The unsymmetrical is isolated from the mixture as a second fraction of liquid column chromatography. This means that the retardation factor of the unsymmetrical is in between the factors of the corresponding symmetrical as in the cases of unsymmetrical and symmetrical TTFs [9,12,16]. The rate of reaction depends on the solvent, the temperature and the nature of R and R'. A number of unsymmetrical complexes of Ni, such as $[Ni(ddd)(edo)]$, $[Ni(ddd)(edo)]$, $[Ni(edo)(ddt)]$, $[Ni(edo)(pdt)]$, $[Ni(edo)(dtm)]$, $[Ni(edo)(dmit)]$ and $[Ni(edo)(mnt)]$ [14] have been prepared by this method.

Scheme 5. Example of a ligand exchange reaction.



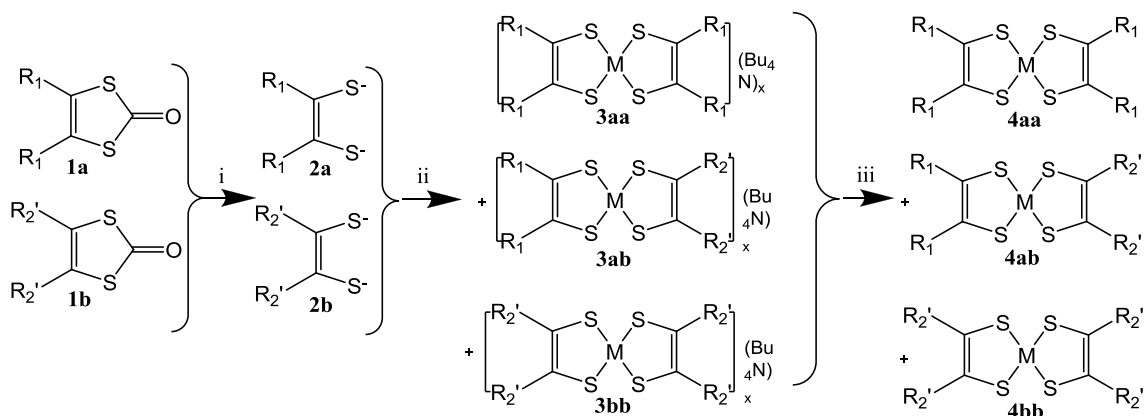
A similar kind of reaction by double substitution of an anionic salt with a cationic at *ca.* 50 °C has been applied to the preparation of unsymmetrical complexes, as in the following Scheme 6.

Scheme 6. Reaction of an anionic and a cationic salt.

By this method a number of the so called push-pull complexes, such as [Ni(H₂pipdt)(dmit)], [Ni(Pr₂pipdt)(dmit)] [Ni(H₂timdt)(dmit)], [Ni(Pr₂timdt)(dmit)] and similarly with mnt instead of dmit have been prepared [80,95].

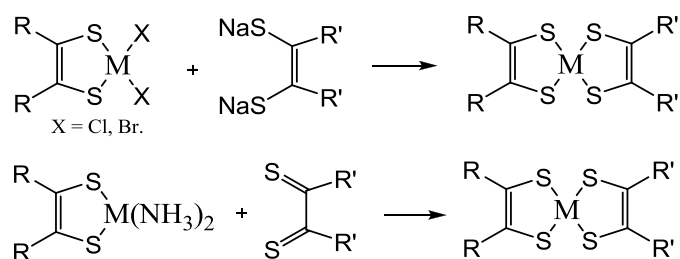
Sometimes, the unsymmetrical complexes prepared by this method were contaminated with the cationic-anionic double salts such as [Pt(Me₂pipdt)₂][Pt(dtc)₂] [15,95,106].

Also, neutral unsymmetrical complexes could be prepared by the so called cross-coupling method, in which ketones are used as starting materials and the neutral complexes were obtained through the corresponding anionic complexes, according to the procedure of the following Scheme 7.

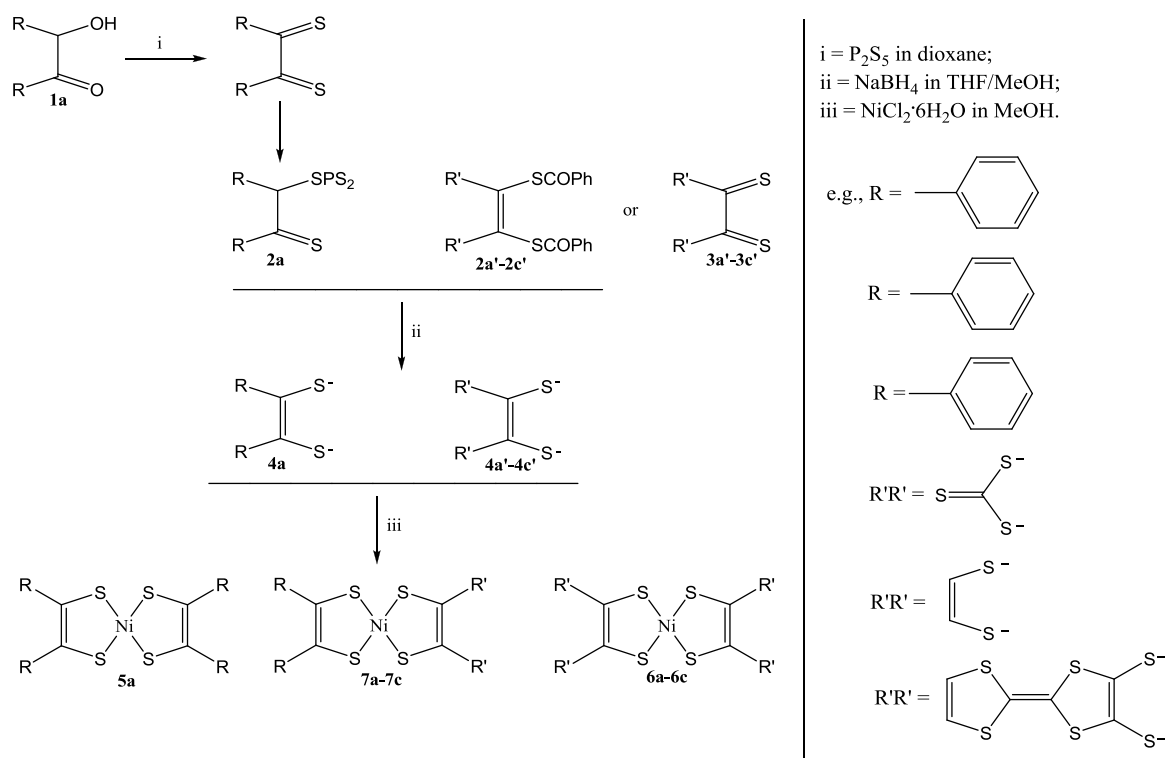
Scheme 7. Cross-coupling procedure for preparation of unsymmetrical complexes.

i = MeONa in MeOH; ii = Bu_4NBr , MX; iii = O_2 (air) in aq. HCl (35%) or Bu_4NI_3 ;
 MX = $NiCl_2 \cdot 6H_2O$, $PtCl_2(PhCN)_2$, $PdCl_2(PhCN)_2$, $NaAuCl_4 \cdot 2H_2O$; x = 2, 1 or $1 > x > 0$.

As in the case of the ligand exchange method, the unsymmetrical complexes are isolated by liquid column chromatography. In some cases the compounds SM1-SM6 and Se analogues as well as, the Zn dianionic compounds (Schemes 2 and 3) instead of 2, have been used to give 3. The advantage of the method is that the reactions take place at room or lower temperatures, and usually the yields are larger than those of the ligand exchange method. A number of neutral complexes, with simple ligands and extended TTF-dithiolato ligands have been prepared by this method: These are [Ni(edt)(ddd)] [27], [Ni(pddt)(dmio)], [Ni(pddt)(dmit)] [36], [Ni(dt)(dmit)], [Ni(dt)(dmio)], [Ni(tmdt)(dmit)], [Ni(tmdt)(dmio)], [Ni(etdt)(dmit)], [Ni(etdt)(dmio)], [Ni(ptdt)(dmit)], [Ni(ptdt)(dmio)], [Ni(dmdt)(dmit)], [Ni(dmdt)(dmio)] [48], [Ni(dmeds)(dmit)], [Ni(dpedit)(dsit)], [Ni(dpedit)(dmit)], [Ni(dcdt)(dmit)] [50], [Pd(dpedit)(ddd)], [Pt(dpedit)(ddd)], [Pd(dpedit)(dmit)], [Au(dpedit)(ddd)] [63], [Ni(tmedt)(ddd)], [Ni(dpedit)(ddd)], [Ni(tmedt)(dmit)], [Ni(dpedit)(dmio)] [64] and [Ni(dpedit)pddt] [94]. Neutral unsymmetrical M 1,2-DTs complexes could be obtained as main products of the reaction of Scheme 8 (see [106] and references therein).

Scheme 8. Some alternative procedures for the preparation of unsymmetrical complexes.

Generally, the cross-coupling method of Scheme 7 gave the unsymmetrical complexes in moderate or low yield. However, a slight modification of the method, in which the deprotection of ligands takes place with NaBH_4 , gave the unsymmetrical complexes obtained in better yield, according to the procedure of Scheme 9 ([12,16,77,101]).

Scheme 9. A modified procedure of cross coupling method.

In these preparations, the starting materials of the types SM1-SM6 could be used instead of 2a'-2c' or 3a'-3c'. The complexes $[\text{Ni}(\text{dpedt})(\text{dmit})]$, $[\text{Ni}(\text{dpedt})(\text{dddt})]$ and $[\text{Ni}(\text{dpedt})(\text{dt})]$ were prepared by this method ([9,48,49] and work in progress). Generally speaking, from a number $N = 100$ ligands of Tables 1–3, one can expect $N(N + 1)/2$ binary combinations, namely 5050 symmetrical and unsymmetrical complexes for each metal, by applying several methods of preparation.

2.2. Growth and Morphology of Crystals

Single crystals suitable for X-ray structure solutions and electrical measurements have been obtained from solutions in organic solvents. It has been found that the vapor diffusion method, using

CS_2 as solvent, and the dilute diffusion method [77,115] using hexane and CS_2 as solvents give good crystals of symmetrical and unsymmetrical M 1,2-DTs [36,50,63,64,79,84]. Also, crystals of neutral complexes with an extended TTF-dithiolato ligand have been obtained by electrooxidation of the corresponding monoanionic or/and the dianionic complexes. (see [22,23,43,45,46]).

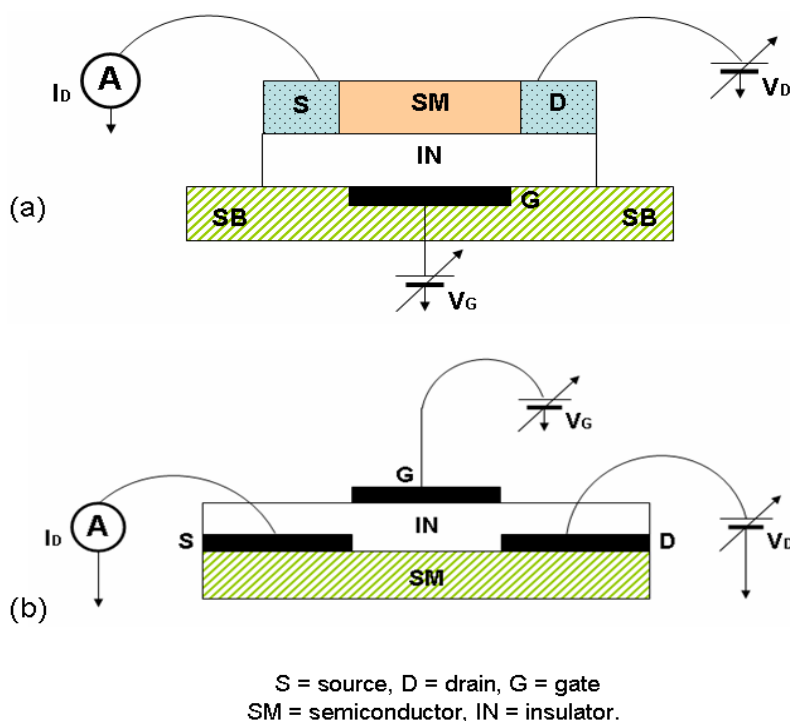
The crystals have a thin needle or thin platelet morphology. From a large number of crystals, only a few of them have been suitable for X-ray structure solution and/or conductivity measurements.

2.3. Instrumentation and Background

The optical absorption (OA), crystal structure (CS), electrical (EL), and electrochemical (ELC) data, described here, were obtained from measurements performed with commercial instruments, the accuracy of which was considered good enough. Consequently, the results obtained by several groups could be compared. The reported conductivity values have been obtained from measurements with the two and/or four-terminal method.

The electrical parameters (e.g., the mobility) under conditions of field-effect transistor (FET) were obtained from two-terminal measurements using the devices of Figure 8. Each of them consists of a gate (G) electrode (e.g., n^+ -Si), a thin dielectric layer (e.g., SiO_2 , parylene), an organic semiconductor (SM) layer (e.g., TTF, M 1,2-DT), a source (S) electrode and a drain (D) electrode (e.g., Al, Ag, TTF TCNQ, Au) on a substrate. Figure 8 shows two types of electrical connections: with bottom-gate, bottom-contact configuration, suitable for polycrystalline deposits (Figure 8a) and with a top-gate, top-contact configuration suitable for single crystals (Figure 8b).

Figure 8. Electrical connections and circuits for measurements under conditions of field-effect transistor (FET): (a) The bottom-gate, bottom-contact configuration (suitable e.g., for polycrystalline semiconducting films) and (b) the top-gate, top-contact configuration (suitable e.g., for single crystal semiconductors) [124,128,129,136].



The system looks like a gate/insulator/channel capacitor, where the channel is the 2-dimensional layer of semiconductor between the S and D electrodes and insulator. When the gate is biased, a current flowing between the S and D electrodes is measured as a function of length (L) and the width (W) of the channel and other parameters concerning the system. The data were used for characterization the system as electron current (n-type system) or hole current (p-type system) and ambipolar (n-type and p-type).

The NLO response of the complexes has been obtained from measurements on homemade apparatus using the Z-scan technique, which allows simultaneous determination of the sign and the magnitudes as both the real (*i.e.*, $\text{Re}\chi^{(3)}$) and the imaginary (*i.e.*, $\text{Im}\chi^{(3)}$) parts of the third-order nonlinear susceptibility $\chi^{(3)}$ of the material in one single measurement with lasers operating in a wavelength of the visible (e.g., 532 nm) or near-IR (e.g., 1064 nm) region [35,48,99,100,111].

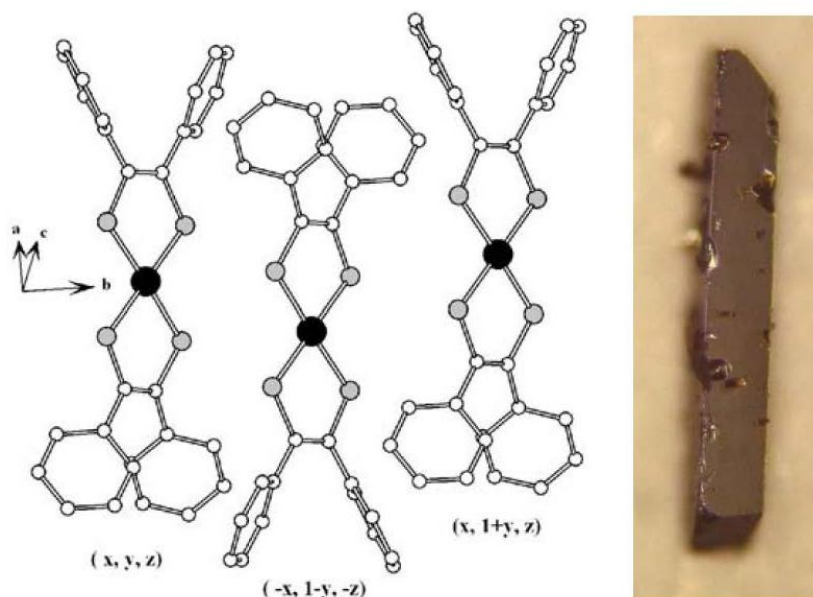
The magnitude of the molecular first hyperpolarizabilities of several unsymmetrical complexes was determined from electric-field induced second harmonic (EFISH) generation experiments usually at 1.9 μm [80,95,106].

3. Structural Properties

In the most neutral M 1,2-DTs, the ligand forms a strictly square-planar arrangement, with all S–M–S bond angles very close to 90°, but with variation in the value of intermolecular S–S contacts. The neutral complexes may exist as planar monomers or form dimers with either metal-metal bonds or metal-sulfur (selenium) bonds. Most of M 1,2-DTs were found to be crystallized in centrosymmetric space group and, up to now, only three complexes have been found to be crystallized in non centrosymmetric space group (see [7,10,15,17,20,63,64,69,94,97]). The data from selected M 1,2-DTs are described here, starting from crystals with weak intermolecular interactions.

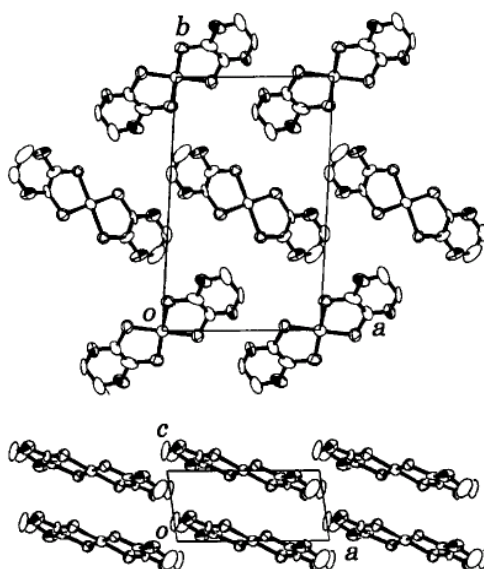
The symmetrical complex α -[Ni(dpdt)₂], for example is crystallized in the centrosymmetric space group P2_{1/n}, where Ni–S = 2.10, C–S = 1.71, C–C = 1.37 Å, S–Ni–S = 89.8, Ni–S–C = 107.3, S–C–C = 118° [3,79]. The symmetrical complex [Au(dpdt)₂] is crystallized in the triclinic space group P1 and is isostructural with β -[Ni(dpdt)₂], but not isostructural with α -[Ni(dpdt)₂], [Pt(dpdt)₂] and [Pd(dpdt)₂] [2,3,7,9]. Figure 9 shows the packing diagram of [Au(dpdt)₂] [79]. In the molecules the Au–S, C–S and the olefinic C–C bond lengths are *ca.* 2.29, 1.73, 1.37 Å, respectively. The bond lengths M–S for the corresponding complexes of several metals (M) increase in the order Au–S > Pd–S > Pt–S > Ni–S. In the cell of [Au(dpdt)₂] the molecules are stacked along the *b*-axis. Both interstacking and intrastacking S–S intermolecular distances are *ca.* 4.5 Å, *i.e.*, much larger than the sum of van der Waal's radii (3.7 Å), while in (Bu₄N)[M(dmit)₂] these distances are 3.59–3.72 Å (see [20] and references therein). This means that the complex has an almost 3D structure, with weak S–S interactions. The long axis of the needle shaped crystals is almost parallel to the *a*-axis. In the samples they have not been found in other habits. Some complexes of the type [Ni(L₉)₂] [56], [Ni(L₆)₂] [61], and similar compounds of Au₂ with ligands containing long chain groups [89,110] are isostructural with [Au(dpdt)₂] [79]. In [Au(bdt)₂], isostructural with α -[Ni(dpdt)₂], the S–S contacts are 3.60–3.66 Å [29].

Figure 9. Packing diagram of a crystal of $[\text{Au}(\text{dpedt})_2]$. Reproduced from [79] with permission from Elsevier, and photograph of a crystal.



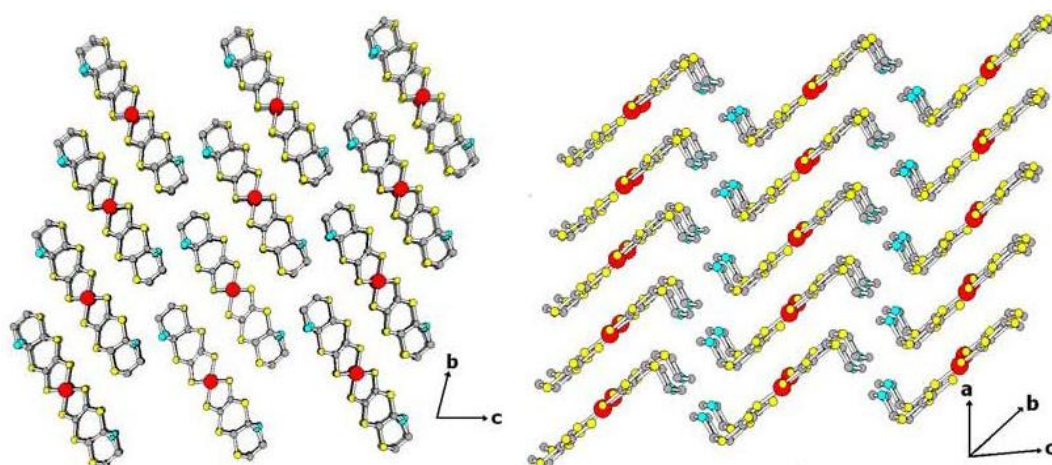
In the structure of symmetrical $[\text{Ni}(\text{dddt})_2]$ [13,14], as in $[\text{Ni}(\text{dmit})_2]$ [69], two molecules (A, B) of the complex form independent uniform stacks along the b -axis. As in the crystal of neutral ET (*i.e.*, BEDT-TTF), there exists a dimer structure. Within the stacks of $[\text{Ni}(\text{dddt})_2]$ the Ni–Ni is 4.67 Å. There is no short intermolecular S–S contact (<3.70 Å) within the stack, and between molecules of adjacent stacks (see [13,14] and references therein). In the structure of the symmetrical $[\text{Ni}(\text{edo})_2]$ (Figure 10) the molecules are planar, as in the case of $[\text{Ni}(\text{dddt})_2]$, while in the corresponding TTFs (*i.e.*, BO and ET) are non-planar. The unit cell of $[\text{Ni}(\text{edo})_2]$ contains two molecules, each of which is repeated uniformly along the c -axis. The Ni–S bond lengths in $[\text{Ni}(\text{edo})_2]$ are slightly larger than that in $[\text{Ni}(\text{dddt})_2]$ (2.12 Å).

Figure 10. Crystal structure of $[\text{Ni}(\text{edo})_2]$. Reproduced from [14] with permission of the Royal Society of Chemistry.



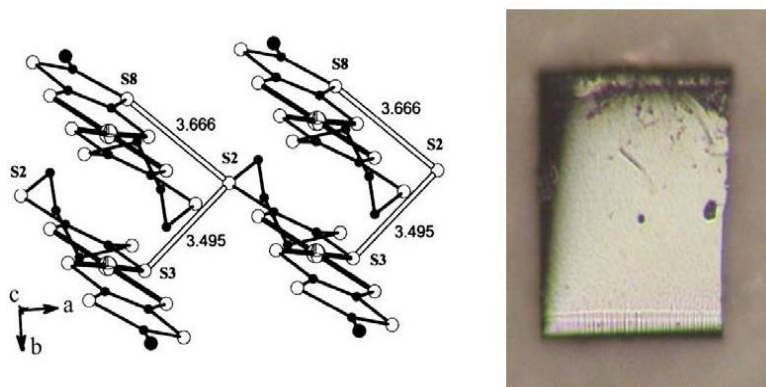
The neutral $[\text{Ni}(\text{dmit})_2]$, studied years ago (see [20,69] and references therein), which is crystallized in plate-like crystals of monoclinic space group $P2_1/a$, show that the molecules stack along the $[010]$ direction, making an angle with the normal to the molecule main plane of 48° . Within the stack, the Ni–Ni spacing is 5.302 \AA and the plane to plane distance 3.562 \AA . In contrast to that observed in the structure of $(\text{Bu}_4\text{N})[\text{Ni}(\text{dmit})_2]$, (see [20,69] and references therein), in the structure of $[\text{Ni}(\text{dmit})_2]$ there are short S–S contacts between adjacent stacks involving the thioacetone sulfur atom (*ca.* 3.58 \AA) [69]. The complex $[\text{Ni}(\text{etoddt})_2]$ (Figure 11) [100] crystallizes in the triclinic space group $P1$, and as in the case of $[\text{Au}(\text{dpedt})_2]$ [79] there are no S–S contacts smaller than the sum of the van der Waals radii.

Figure 11. Schematic presentation of the structure of $[\text{Ni}(\text{etoddt})_2]$.



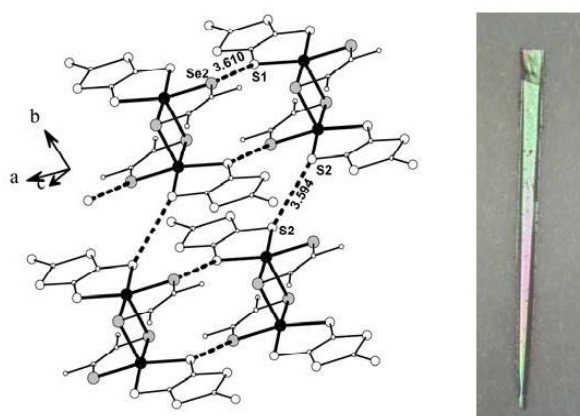
The unsymmetrical complexes $[\text{Ni}(\text{pddt})(\text{dmio})]$, $[\text{Ni}(\text{tmedt})(\text{ddd})]$, and $[\text{Ni}(\text{tmedt})(\text{dmit})]$ are isostructural and crystallized in the monoclinic space group $P2_1/c$ [36,64]. Figure 12 shows a perspective view of the $[\text{Ni}(\text{pddt})(\text{dmio})]$ structure and a photograph of the crystal. In a layer almost parallel to the ab -plane there are S–S intermolecular contacts of 3.49 and 3.66 \AA . In the other directions the distances are larger. In $[\text{Ni}(\text{tmedt})(\text{ddd})]$ and $[\text{Ni}(\text{tmedt})(\text{dmit})]$ these contacts are 3.59 and 3.70 – 3.73 \AA , respectively. The intermolecular contacts form a quasi-two-dimensional (q-2D) network. It was found that the largest surface of the crystal is parallel to the crystallographic ab -plane.

Figure 12. Perspective view of the $[\text{Ni}(\text{pddt})(\text{dmio})]$, reproduced from [36] with permission of the Verlag der Zeitschrift für Naturforschung, and photograph of crystal [77].



The complex $[\text{Ni}(\text{dmeds})(\text{dmit})]$ crystallizes in the triclinic space group $P1$. Figure 13 shows that the partial labeled plot of complex showing the intermolecular contacts [50]. The structure consists of centrosymmetric dimers [7] with the inversion center sitting on the center of the Ni_2Se_2 core. The closest Ni–S and Ni–Se bond lengths in the coordination sphere are *ca.* 2.2 and 2.3 Å respectively, while the longer Ni–Se bond (2.56 Å) is responsible for the formation of the dimers. The closest intramolecular Ni–Ni distance is *ca.* 3.06 Å. It was found that the largest surface of the rectangular crystals is almost parallel to the crystallographic *ab*-plane. There are S–S and S–Se intermolecular contacts of 3.594 and 3.560 Å, respectively, slightly smaller than the sums of van der Waals radii (3.70 and 3.82 Å, respectively), which give rise to the formation of layers almost parallel to the *ab*-plane. In other directions the distances are larger. This indicates a *quasi* two dimensional behavior of the material.

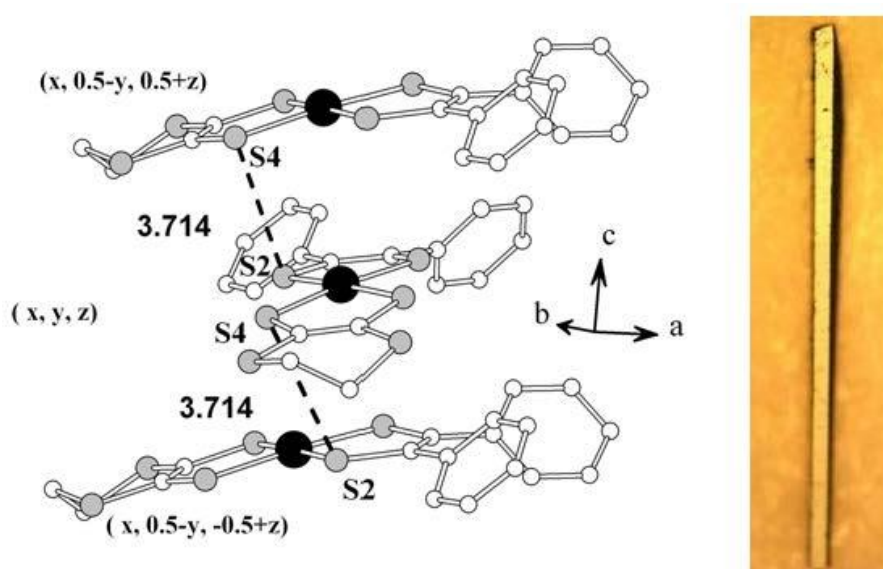
Figure 13. Partial labeled plot of $[\text{Ni}(\text{dmeds})(\text{dmit})]$, reproduced from [50] with permission of the Verlag der Zeitschrift für Naturforschung, and photograph of crystal [77].



The unsymmetrical complexes $[\text{Pd}(\text{dpedt})(\text{dddt})]$, $[\text{Ni}(\text{dpedt})(\text{dddt})]$ and $[\text{Ni}(\text{dpedt})(\text{pddt})]$ are isostructural and are crystallized in the orthorhombic non-centrosymmetric space group $Pbc2_1$ [63,64,94]. Figure 14 shows the stacking of $[\text{Pd}(\text{dpedt})(\text{dddt})]$ molecules in a column along the *c*-axis. However, there is no pseudocentro-symmetrical arrangement of molecules [20]. It was found that the needle axis of the crystal is the *c*-axis. The shortest S–S distance in $[\text{Pd}(\text{dpedt})(\text{dddt})]$ is 3.714 Å. The intermolecular contacts form a q-1D network. In $[\text{Ni}(\text{dpedt})(\text{dddt})]$ [64] and $[\text{Ni}(\text{dpedt})(\text{pddt})]$ [94] these distances are 3.764 and 3.738 Å, respectively, which are a little larger than the sums of van der Waals radii (3.70 Å).

In some cases of unsymmetrical M 1,2-DTs, where one of the ligands has a push character (dithione) and the other a pull character (dithiolate), the C–S and C–C distances in the two ligands are different [31,80,95]. For example, in $[\text{Ni}(\text{Pr}_2\text{timdt})(\text{dmit})]$, the C–S and C–C distances for the ligand Pr_2timdt are 1.69 and 1.38 Å, while for the ligand dmit the distances are 1.74 and 1.29 Å, respectively. In $[\text{Ni}(\text{tmedt})(\text{dddt})]$ the push/pull character is weak and the corresponding values for tmedt are 1.68 and 1.37 Å, while for dddt are 1.71 and 1.38 Å [64,95]. Similar results as in $[\text{Ni}(\text{tmedt})(\text{dddt})]$ have been obtained from non centrosymmetric complexes $[\text{Pd}(\text{dpedt})(\text{dddt})]$ [63], $[\text{Ni}(\text{dpedt})(\text{dddt})]$ [64] and $[\text{Ni}(\text{dpedt})(\text{pddt})]$ [94].

Figure 14. Crystal structure of [Pd(dpdt)(dddt)]. Reproduced from [63] with permission of the Verlag der Zeitschrift für Naturforschung, and photograph of crystal [77].



In [Ni(dt)(dmit)] and similar complexes with one extended TTF dithiolate ligand there are no crystallographic data. The IR vibrational spectra of [Ni(dt)(dmit)] indicate a dithioglyoxal structure (large HC–CH bond) in the dt ligand of this complex, rather than an olefinic structure (short HC–CH bonds) as in the edt ligand of [Ni(edt)₂] [49], and consequently, a push/pull behaviour in [Ni(dt)(dmit)] and similar compounds [48,89]. It is suggested that the molecular structure has a resonance form similar to that of the push/pull complexes [95].

In the structure of [Ni(edo)(dmit)], the almost planar molecules are repeated in band to tail fashion along the *c*-axis. The average bond lengths of Ni–S, C–S, and C–C are 2.15, 1.70 and 1.39 Å, respectively. In the structure of [Ni(edo)(mnt)], the molecules are arranged alternately along the *c*-axis. The average bond lengths of Ni–S, C–S, and C–C are 2.15, 1.62 and 1.32 Å, respectively. In the crystal structure of Cu(dmdt)₂, the molecules are not planar [25]. The ligands have an arrangement similar to that of κ -phase TTFs based organic conductors and superconductors [12].

The complex [Ni(tmdt)₂], which is based on the extended TTF dithiolate ligand, tmdt, crystallizes into a very simple and compact structure, the triclinic space group P $\bar{1}$. The molecules are planar and form a close packed structure. The S–S contacts are 3.44–3.75 Å. The structural features suggest that the complex is a three-dimensional (3D) anisotropic solid [46]. The complexes [Au(tmdt)₂] and [Pt(tmdt)₂] [90] are isostructural with [Ni(tmdt)₂] [45,46].

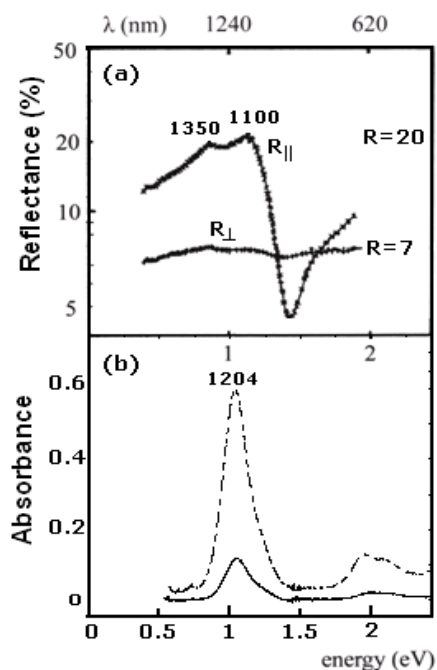
Briefly, the examples of structures given herein and those described elsewhere (see [9–114] and references therein) show the existence of a variety of three and low dimensional networks formed from short or large M–S, S–S, *etc.* contacts. The nature of the individual molecules plays an important role in the unique intermolecular interactions. From the crystallographic data and the transfer integrals the electronic band structure could be calculated [18,20,51]. Consequently, it is expected that there is also a wide variety in behavior, concerning electronic (see [7,18]) and other (see [2–4,6–15,17,19–114]) properties of M 1,2-DTs, in the solid state.

4. Optical Properties

The optical properties of M 1,2-DTs in the form of single crystals, polycrystalline pellets, thin film (or deposits), suspensions, composites and solutions have been reported in a number of papers. It was observed, years ago, that the optical absorption (OA) spectra of solutions of monoanionic M 1,2-DTs (M = Ni, Pd, Pt), which are paramagnetic compounds, exhibit strong bands, which span the range 700 to *ca* 1900 nm, depending on the nature of the metal, the ligand and the solvent (see for examples [10,18,34,63,70]). The bands have been interpreted as the HOMO-LUMO transitions or as ligand-to-ligand (LL) charge transfer (CT) transitions [34,95]. These bands and the bands of the isoelectronic neutral Au 1,2-DTs have an unsymmetrical shape. After a Gaussian deconvolution it has been found that the bands are dominated by two transitions: one intense at low frequency is assigned to $1b_{1u} \rightarrow 2b_{2g}$ (*x*-polarized) and one medium to $1a_{1u} \rightarrow 2b_{2g}$ (*y*-polarized), as well as some weaker ones [18,34]. The experimental values of transitions, *i.e.*, the band position and intensity of OA bands, have been found to be in reasonable agreement with the theoretically calculated ones [18,34]. The splitting of the low frequency band is more discreet in the OA (and reflectance) spectra of the complexes in the solid state (see for example [29] and refs. [9–11] cited therein).

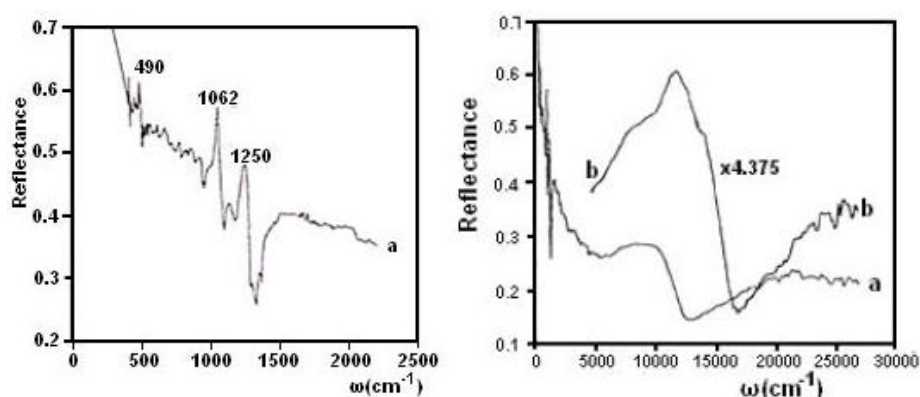
Figure 15 shows the polarized reflectance spectra of $(\text{Bu}_4\text{N})[\text{Ni}(\text{dmit})_2]$ with the wavevector of the light parallel (R_{\parallel}) and perpendicular (R_{\perp}) to the needle axis of the crystal, as well as the OA spectra of the material in CS_2 solution and a suspension in CCl_4 . The reflectance spectra show anisotropic behavior due to the low dimensional structure of the material [20,120]. In parallel polarization the band is split into two sub-bands at 1100 and 1350 nm. The reflectance spectrum of a polycrystalline pellet shows the same bands, while the spectra of a suspension of the material in CCl_4 and that of the solution in CS_2 show narrow bands at *ca.* 1204 nm, with an unsymmetrical shape.

Figure 15. Polarized reflectance spectra of $(\text{Bu}_4\text{N})[\text{Ni}(\text{dmit})_2]$, optical absorption (OA) spectrum of a suspension of material in CCl_4 (solid line) and of solution in CS_2 (dashed line) [77].



Different results have been obtained from cation deficient complexes. The reflectance spectra of polycrystalline pellets of $(\text{Bu}_4\text{N})_x[\text{Ni}(\text{dmit})_2]$ and $(\text{Bu}_4\text{N})_x[\text{Pt}(\text{dmit})_2]$, obtained after oxidation of monoanionic salts with iodine or bromine [6,12,47], are shown in Figure 16. In these cation-deficient complexes (which behave as mixed-valence complexes) with $x = 0.25$ and $x = 0.2$, respectively, the low frequency band-position, -intensity, and -shape depend on the x -value. When $x \rightarrow 0$, the (neutral) complex exhibits a narrow band, blue shifted from that of monoanionic ($x = 1$), while for intermediate values of x , the complex exhibits a new band at lower frequencies. The reflectance spectra of Figure 16 seem to be the superposition of those of a mixture of cation-deficient and neutral complexes. Strong OA bands of cation deficient complexes $(\text{Bu}_4\text{N})_{0.06}[\text{Au}(\text{eddt})_2]$, $(\text{Bu}_4\text{N})_{0.4}[\text{Pt}(\text{eddt})_2]$ and $(\text{Bu}_4\text{N})_x[\text{Au}(\text{dmit})_2]$ occur at *ca.* 860 nm [40], close to that of $(\text{Bu}_4\text{N})_{0.2}[\text{Pt}(\text{dmit})_2]$.

Figure 16. Reflectance spectra of polycrystalline pellets of $(\text{Bu}_4\text{N})_x[\text{Ni}(\text{dmit})_2]$ (a); $(\text{Bu}_4\text{N})_x[\text{Pt}(\text{dmit})_2]$ (b). Reproduced from [54] with permission from Elsevier.



The OA spectra of neutral complexes exhibit strong bands, the position of which depends strongly on the nature of the metal, the ligand the solvent, *etc.* The OA band positions (and intensities) of unsymmetrical complexes (AB) in solutions occur in between those of the corresponding symmetrical complexes (AA, BB). The characteristic OA wavelength (maximum or onset) is given by the equation:

$$\lambda_{(\text{AB})} = [\lambda_{(\text{AA})} + \lambda_{(\text{BB})}]/2 \quad (1)$$

Figure 17 shows the experimentally observed spectra of $[\text{Ni}(\text{edt})_2]$, $[\text{Ni}(\text{edt})(\text{dddt})]$ and $[\text{Ni}(\text{dddt})_2]$ solutions in MeOH [27]. The observed OA band of the unsymmetrical $[\text{Ni}(\text{edt})(\text{dddt})]$ occurs at 864 nm while, the calculated from those of symmetrical and Equation 1 was found at 867 nm.

The OA band position of neutral $[\text{Ni}(\text{dmit})_2]$ in solution has been calculated from the positions of the corresponding bands of some symmetrical $\text{Ni}(\text{L})_2$ and unsymmetrical $[\text{Ni}(\text{L})(\text{dmit})]$ complexes using Equation 1. It has been found to be *ca.* 1070 nm in CS_2 and 1043 nm in CH_3CN . The calculated value for $[\text{Ni}(\text{dmio})_2]$ is 932 nm in CS_2 . The OA spectra of some Au-based complexes and the OA band position of Pd-based complexes in CS_2 are shown in Figure 18. It can be seen that the Au-materials exhibit wide transparent spectral regions, *i.e.*, from *ca.* 500 nm to *ca.* 1500 nm. It was found that the spectra of $[\text{Au}(\text{tmedt})(\text{dddt})]$ and $[\text{Au}(\text{tmedt})_2]$ in CS_2 exhibit OA bands at *ca.* 1732 and 1500 nm, respectively. Generally, the OA bands of neutral Au 1,2-DTs occur at lower frequencies, even, than those of monoanionic salts of Ni, Pd and Pt, which are isoelectronic

(see Figures 17 and 18 for examples) [63,70]. The OA and reflectance bands of single crystals of $[\text{Au}(\text{bdt})_2]$ occur close to 2000 nm [29].

Figure 17. UV-vis/near IR absorption spectra of $[\text{Ni}(\text{dddt})_2]$ (a); $[\text{Ni}(\text{edt})_2]$ (b) and $[\text{Ni}(\text{dddt})(\text{edt})]$ (c) in MeOH. Reproduced from [27] by permission of the Verlag der Zeitschrift für Naturforschung.

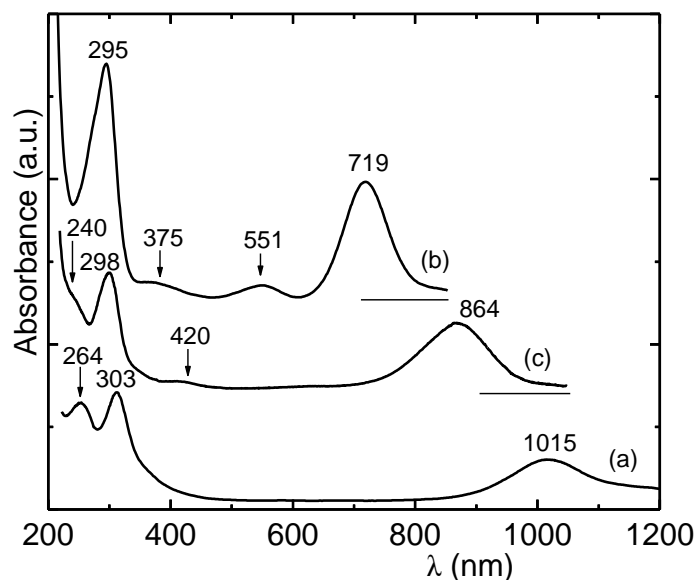
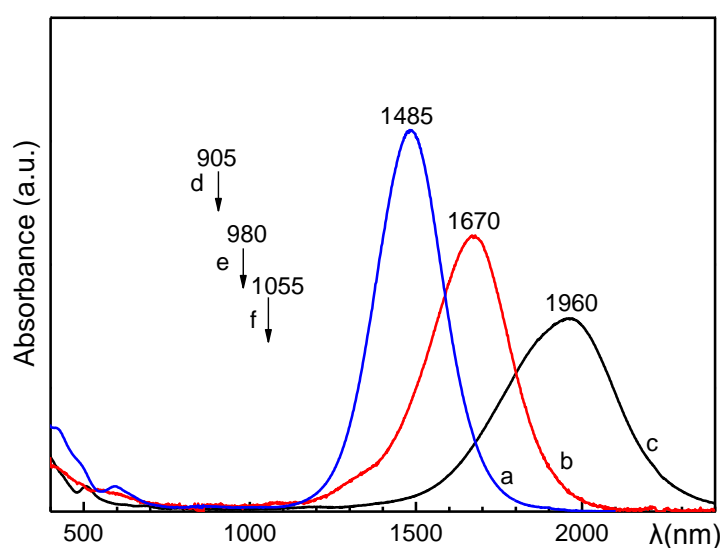


Figure 18. OA spectra of $[\text{Au}(\text{dpedt})_2]$ (a), $[\text{Au}(\text{dpedt})(\text{dddt})]$ (b) and $[\text{Au}(\text{dddt})_2]$ (c): arrows indicate the OA band positions of $[\text{Pd}(\text{dpedt})_2]$ (d) $[\text{Pd}(\text{dpedt})(\text{dddt})]$ (e) and $[\text{Pd}(\text{dddt})_2]$ (f) in CS_2 [63,70].



The OA spectra of unsymmetrical M 1,2-DTs with a push-pull behavior, such as $\text{M}(\text{Bz}_2\text{pipdt})(\text{mnt})$ [95,106], exhibit broad bands at *ca.* 751 (660sh), 651 (560sh) and 685 nm in DMF for $\text{M} = \text{Ni}$, Pd , and Pt , respectively, with low to medium molar absorption coefficient and negative solvatochromism [106]. The OA spectra occur between the spectra of the corresponding symmetrical (if they exist), but do not obey Equation 1. Similar results have been obtained from

[Pd(Me₂Pipdt)(dmit)] [88] solutions in DMSO. In solution four peaks are present, and that at 737 nm may be tentatively assigned to the HOMO-LUMO transition. This band shows negative solvochromism and occurs at higher energy, when compared to the one in the corresponding Ni compound (910 and 965 nm respectively, in CHCl₃).

The position, intensity and shape of the bands in the solid state (single crystals, polycrystalline pellets, thin deposits, *etc.*) depend on the structural feature of the complex. If the S–S contacts, for example, are weak as in [Au(dpedit)₂], the position of the OA band of a thin film occurs close to that of the solutions, while, if the S–S contacts are strong as in the [Au(dddt)₂] and [Au(bdt)₂] [29], the OA bands occur at lower frequencies.

As in the OA spectra of charge transfer (CT) and mixed valence (MV) compounds (see [117,120]), the OA onsets or the E_g values of single component species (i), including small particles of M 1,2-DTs could be obtained from the following Equation 2,

$$(E_g)_i = \Delta E - 2(t_1)_i - 2(t_2)_i \quad (2)$$

where ΔE is the HOMO/LUMO gap, $(t_2)_i$ and $(t_1)_i$ the corresponding intermolecular transfer integrals. These integrals could be obtained from band structure calculations based on crystallographic data. Figure 19 shows the schematic presentation of bands and gap $(E_g)_i$ formation from a one dimensional array of neutral molecules with HOMO/LUMO (H, L) gap of ΔE , where $(t_1)_i$ and $(t_2)_i$ are the corresponding transfer integrals, for any species (i) concerning bulk (large t) and small particles (small t). If the structure results from dimers, the energy gap is lower than the corresponding levels of dimers [7,21,51]. Figure 20 shows the OA spectra of thin deposits of [Au(dpedit)₂], [Au(dpedit)(dddt)] and [Au(tmedit)₂] obtained by rubbing the complexes on quartz plates. Because of the weak intermolecular interactions in the solid state [63,79], the bands occur almost at the same positions as those of the solutions, but are broader, and the fine structure is not clear. The same OA spectra have been obtained from suspensions of the complex in CCl₄ or toluene and from composites of the complex in a polymethylmethacrylate matrix. However, the spectra of films, obtained by a spin-coating technique, showed a fine structure [79], which could be attributed to several molecular transitions [34]. However, in the cases of [Ni(etdt)₂] [77], [Ni(dt)(dmit)] [49], [Ni(dmdt)(dmio)] [48] and [Ni(dmstfdt)(dmio)] [48] the differences between the spectra of deposits and those of solutions are larger, because of the stronger intermolecular interactions in the solid state. Figure 21 shows the OA spectra of [Ni(etdt)₂] thin deposits before (a) and after (b) rubbing as well as the spectrum of a solution in CS₂ (c), for comparison. Figure 22 shows the spectra of thin deposits of [Ni(dmdt)(dmio)] and [Ni(dmstfdt)(dmio)]. It can be seen again that after extensive rubbing, the bands occur close to those of the solutions, which indicates weak interactions [134].

Figure 19. Schematic presentation of the bands and gap (E_g)_i formed from the HOMO/LUMO levels [7,12,21,51].

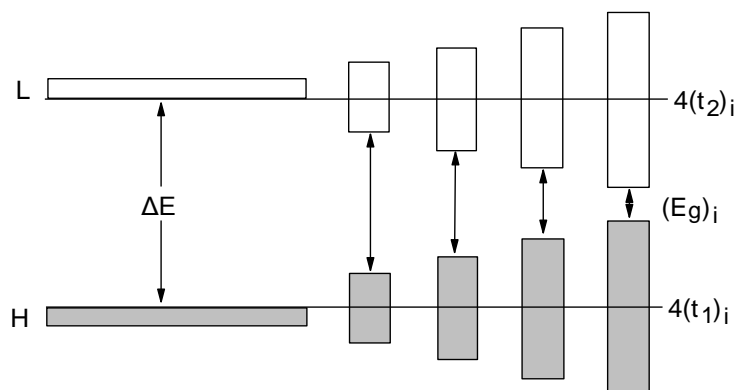


Figure 20. OA spectra of thin deposits of [Au(dpdt)₂] (a) [Au(dpdt)(dddt)] (b) and [Au(tmedt)₂] (c) obtained by rubbing the materials on quartz plates [77,79].

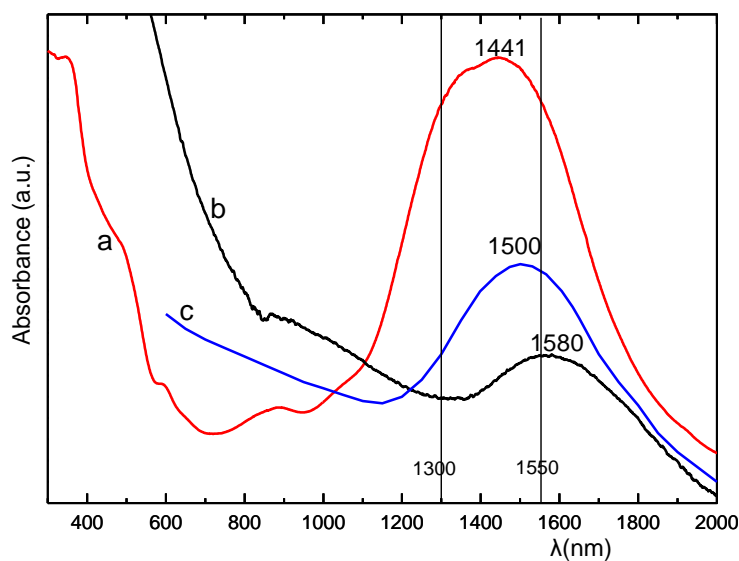


Figure 21. OA spectra of thin deposits of [Ni(etdt)₂] before (a) and after (b) rubbing on a quartz plate and the OA band of a solution in CS₂, for comparison (c) [77].

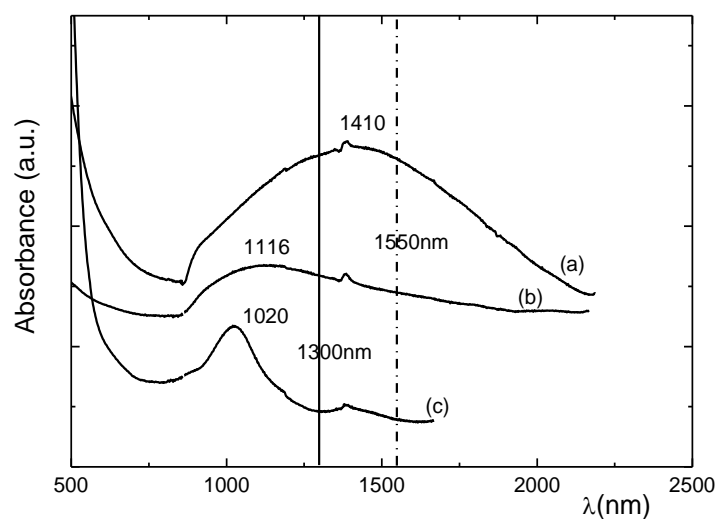
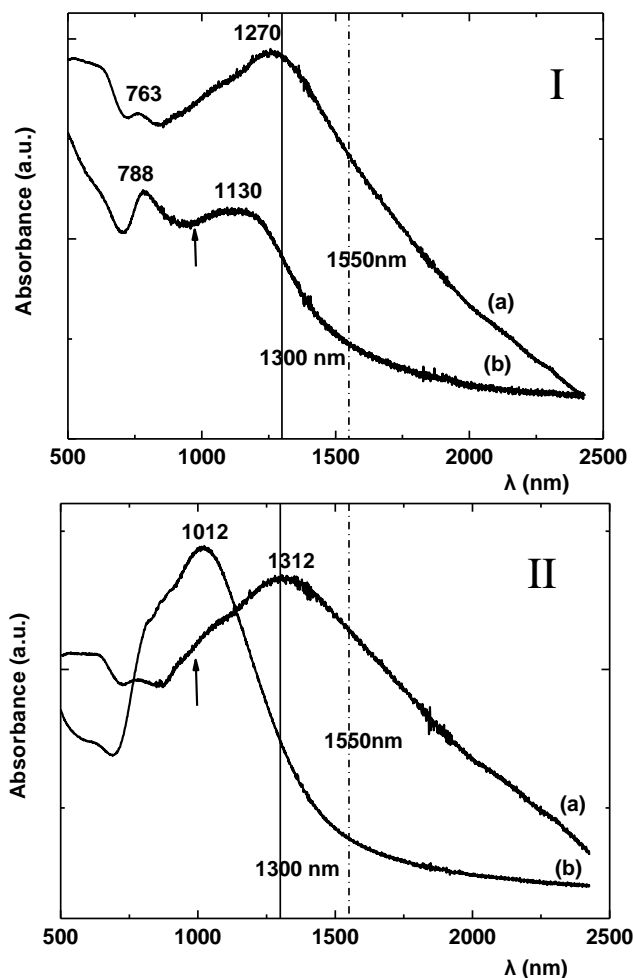


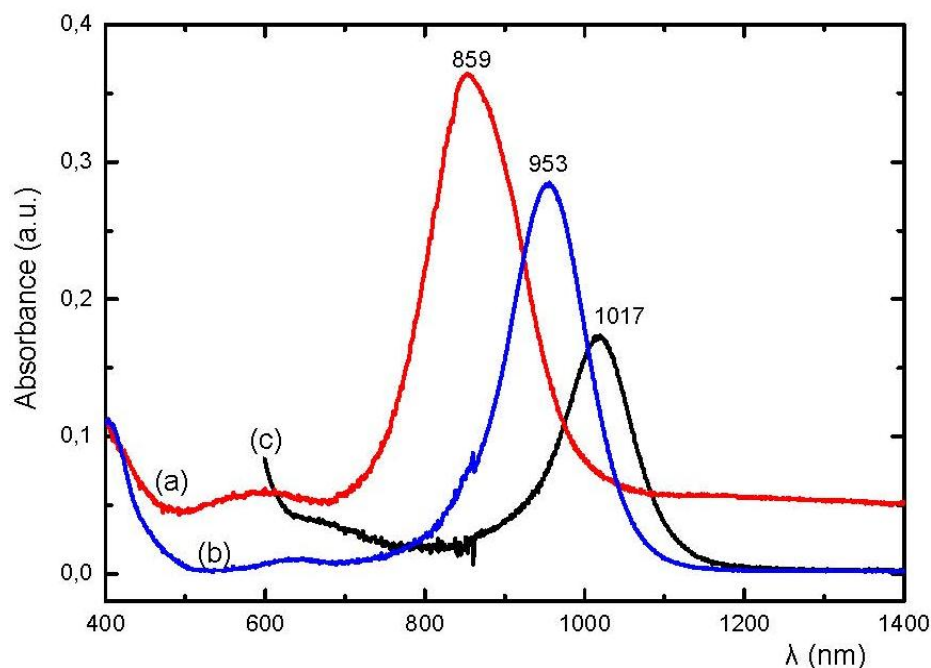
Figure 22. Panel I. OA spectra of thin deposits of [Ni(dmdt)(dmio)] before (a) and after (b) rubbing on a quartz plate. The arrow indicates the OA band-position of a solution in CS₂. Panel II. same as panel 1, except for [Ni(dmstfdt)(dmio)]. Reproduced from [48] by permission of the Verlag der Zeitschrift für Naturforschung.



The spectral behavior of [Ni(etdt)₂], [Ni(dmdt)(dmio)], [Ni(dmstfdt)(dmio)], as well as that of [Au(bdt)₂] [29], reminds us of similar effects observed in the CT complexes such as KTCNQ [117] and mixed valence complexes of the type X–M–X (where X = Cl, Br, I; M = Pt, Pd, Ni) [118].

The OA spectra of suspensions of neutral M 1,2-DTs occur close to those of the corresponding solutions and obey Equation 1. As an example, the spectra of suspensions of [Ni(dmit)₂], [Ni(dpedit)₂] and [Ni(dpedit)(dmit)] in CCl₄ are given in Figure 23. The neutral [Ni(dmit)₂], has been prepared in single crystal form [69] and could be obtained in suspension form by injection of (Bu₄N)_x[Ni(dmit)₂] solution in CS₂ into CCl₄ containing I₂, under vigorous stirring [6,12]. The calculated OA band position of [Ni(dmit)₂] from the corresponding band positions of [Ni(dpedit)₂] and [Ni(dpedit)(dmit)] is 1047 nm, while the observed experimental value is 1017 nm ([50,54] and work in progress). This is close to the calculated (above) for the spectrum of [Ni(dmit)₂] in CH₃CN-solution.

Figure 23. OA spectra of suspensions of [Ni(dpdt)₂] (a), [Ni(dpdt)(dmit)] (b) and [Ni(dmit)₂] (c) in CCl₄ [77].



A large difference in the band positions and deviation from Equation 1 was observed in the spectra of extended-TTF dithiolato ligands [45,46]. For example, the OA spectra of solutions of [Ni(dmdt)₂] and [Ni(dmdt)(dmit)] in CS₂ show bands at 985 and 1037 nm, respectively. The OA band position of [Ni(dmdt)₂] calculated from Equation 1, occurs at 1089 nm. However, in the solid state, because of the strong interactions in [Ni(dmdt)₂] [32,45,46,134], the low frequency band occurs at *ca.* 4545 nm [46]. In other words, the OA-band positions and shapes of M 1,2-DTs, such as [Ni(etdt)₂] and [Ni(ptdt)₂], with strong intermolecular interactions vary from sample to sample in the solid state (Figures 20–22 and Table 4). The reflectance spectrum of [Pd(Me₂pipdt)(dmit)], except for the main peak at *ca.* 737 nm, shows an additional peak which could be attributed to an intermolecular transition involving the dmit moieties interacting through short S–S intermolecular contacts [88].

Table 4. Optical absorption (OA) band position (nm) and OA onsets (eV), of a number of selected M 1,2-DTs.

Complex	Solvent		Thin deposit			E ^{opt} _{onset}
	CS ₂	CH ₂ Cl ₂	(a)	(b)	(c)	
[Ni(edo) ₂]		853				(1.34)
[Ni(dpdt) ₂]	875					(1.18)
[Ni(dmedt) ₂]	788					(1.36)
[Ni(ddt) ₂]	1033					(1.1)
[Ni(didt) ₂]	1007					(0.85)
[Ni(dmvdt) ₂]	1167					(1.0)
[Ni(dddtd) ₂]	1033			1119		0.62 (1.0)
[Ni(tmdt) ₂]	1005		4545			0.25 (1.0)
[Ni(dmdt) ₂]	978		4545			0.25 (1.0)
[Ni(etdt) ₂]	1020		1410	1116		0.68 (1.25)
[Ni(ptdt) ₂]	1027	1000	2127			0.55 (1.0)

Table 4. Cont.

[Pd(dpedit) ₂]	905					(1.18)
[Pd(ddd) ₂]	1055					(1.0)
[Pd(dt) ₂]			1289			(0.20)
[Pt(dpedit) ₂]	918					(1.37)
[Pt(ddd) ₂]	987					(1.15)
[Au(dpedit) ₂]	1485		1441			0.82 (0.82)
[Au(ddd) ₂]	1960					(0.55)
[Au(tmedt) ₂]	1500		1510			0.8 (0.08)
[Ni(edt)(ddd)]	894	870	954	893		1.02 (1.2)
[Ni(edt)(dmio)]	830	810		803		1 (1.15)
[Ni(edt)(dmit)]	906	875				(1.15)
[Ni(dmedt)(dmio)]	866	840				(0.95)
[Ni(dmedt)(dmit)]	933	901		870		1.02 (1.15)
[Ni(dpedit)(pddt)]	947			981		1.0 (1.08)
[Au(dpedit)(ddd)]	1670		1580			0.6 (0.63)
[Pt(dpedit)(ddd)]	906			1037		1.12 (1.2)
[Ni(dmeds)(dmit)]	950		914			1.03 (1.13)
[Ni(dpedit)(dsit)]	1005					(1.0)
[Ni(tmedt)(dmio)]	838	800				
[Ni(tmedt)(dmit)]	945		1035	965	1120	0.79 (1.2)
[Ni(tmedt)(ddd)]	936	922	1020	1020	1058	0.89 (1.2)
[Ni(pddt)(dmio)]	978		921	935		0.8 (1.2)
[Ni(pddt)(dmit)]	1035	1003	950	933		0.78 (1.0)
[Ni(ddd)(dmio)]	978					(1.0)
[Ni(ddd)(dmit)]	1040					(1.12)
[Ni(mddd)(dmit)]	1039					
[Ni(dpedit)(dmio)]	906	884	897			0.99 (1.25)
[Ni(dpedit)(dmit)]	974	945	1007	940	1050	0.92 (1.1)
[Pd(dpedit)(dmit)]	1000			1022		0.88 (1.10)
[Pd(dmedt)(dmio)]	955	925				(1.15)
[Pd(dmedt)(dmit)]	1067					(1.07)
[Pd(dpedit)(ddd)]	980			1038		1.10 (1.12)
[Ni(dpedit)(ddd)]	955	933	1059	1058	1025	0.83 (1.06)
[Ni(dcdt)(dmit)]	1040	1004	999	1003	1025	0.74 (1.0)
[Ni(dt)(dmio)]	978		1245	1175		0.72 (1.05)
[Ni(dt)(dmit)]	1039		1245	1170		0.73 (1.03)
[Ni(dmdt)(dmio)]	977		1270	1130		0.70 (1.0)
[Ni(dmdt)(dmit)]	1037		1260	1170		0.72 (1.0)
[Ni(tmdt)(dmio)]	978		1250	1000		0.82 (1.2)
[Ni(tmdt)(dmit)]	1046		1360			0.72 (1.0)
Ni(dmstfdt)(dmio)]	988		1312	1012		0.83 (1.2)
[Ni(etdt)(dmio)]	982		1250			0.82 (1.06)
[Ni(etdt)(dmit)]	1035	1015	1300	1150		0.72 (1.0)
[Ni(pddt)(dmio)]	978		1238	1170		0.73 (1.13)
[Ni(pddt)(dmit)]	1041		1260			0.71 (1.0)

OA band position of thin deposits obtained by drop-casting (a); grinding rubbing (b) and spin-coating (c) techniques. Optical onset values from the spectra of solutions in CS₂ are given in parentheses.

Table 4 gives the OA band positions and onsets in a number of selected M 1,2-DTs in solutions (CS_2 , CH_2Cl_2) and in the solid state, which give information on the LUMO-HOMO gap and the energy gap of material in the solid state ($E_g^{\text{op}} = E_{\text{onset}}^{\text{op}}$), respectively. One can see that this last parameter varies from 0.62 to *ca.* 1 eV. The values of OA onsets were obtained from the OA spectra of thin deposits. This means that the corresponding values from bulk materials (*i.e.*, single crystals) should be smaller. On the other hand, the values obtained from very thin deposits (and suspensions) will be larger and close to those of solutions. In these cases the OA band positions of unsymmetrical and corresponding symmetrical obey Equation 1. In the push-pull complexes the E_g -value is *ca.* 1.5 eV (830 nm), while in complexes with extended-TTF dithiolato ligands this is small ($\ll 0.6$ eV).

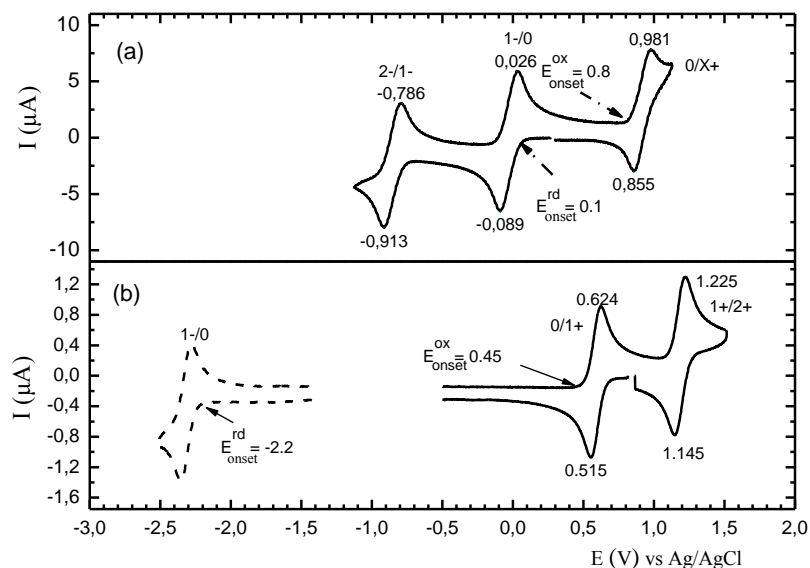
The spectra of Figures 18 and 20–22 show that the complexes have significant absorption maximum near the telecommunication laser wavelengths (*i.e.*, 1300 and 1550 nm). This is a requirement, which dyes have to meet to be usable as optical filters, saturable absorbers, Q-switches and mode-lockers (see for example [10,24,31,76,121]). Because of the wide transparent range, the band position, shape and intensity as well as the stability in air, illumination of solutions of complexes with high power lasers exhibit some other significant non-linear optical (NLO) properties [20,35,48,58,63,64,67,80,94,95,99,100,103,106,111]. For example, using solutions of symmetrical or unsymmetrical M 1,2-DTs the second hyperpolarizability γ has been observed to be as large as 10^{-27} esu [35]. Also, from solutions of unsymmetrical complexes of the type push-pull, a large value in the (negative) second polarizability (β) has been observed [106]. However, for similar observations concerning second harmonic generation from solid materials there is no information. Although, there are known complexes with noncentrosymmetrical structures [63,64,94], in these structures the molecules do not have a pseudo-centrosymmetric arrangement [20].

5. Chemical and Electrochemical Properties

The chemical and electrochemical reactivities, mainly of homoleptic M 1,2-DTs, reported before 2004, have been summarized in [8,19,24]. For results concerning new ligands and structures see [17–114]. Also, for a wide range of electrochemical aspects of molecular solids see [122]. Examples, concerning chemical reactivity, are ligand exchange reactions as well as ligand addition and substitution reactions. Methods of preparations of neutral and unsymmetrical complexes, based on these kinds of reactions, have been already described in section 2. The selection of reactions as well as the selection of oxidizing, or reducing agents for the preparation of stable (in air) complexes are related to the electrochemical (redox properties) of the materials. The cyclic voltametry (CV) measurements of M 1,2-DTs provide useful electrochemical parameters. These are the half wave redox potentials, defined as $E_{1/2}(i) = [E_{\text{ox}}(i) + E_{\text{red}}(i)]/2$, where $E_{\text{ox}}(i)$ and $E_{\text{red}}(i)$ are the oxidation and reduction potentials of several redox couples ($i = 2-/1-$, $1-/0$, *etc.*), respectively. These parameters play an important role in the formation, stability and other properties of M 1,2-DTs and their salts. Figure 24 shows a schematic presentation of a voltammogram of a M 1,2-DT and that of a donor molecule, *e.g.*, of a TTF compound, for comparison. One can see that there are some common features at their positive potentials, which lead to the formation of cationic salts in both cases [16,21]. The couple $E_{1/2}(0/x+)$ ($0 < x \leq 1$) is rare [79,95]. Instead of which, an irreversible wave $E(0/x+)$ is observed. However, in the negative potentials there are considerable differences: the couples concerning $1-/0$ (or $2-/1-$) states are absent or rare in the voltammograms of donor molecules [12,16]. These couples

are observed in the voltammograms of acceptors, e.g., of TCNQ (0.17, -0.37 V vs. SCE), and TCNQ(CN)₂ (1.31, 0.51 V vs. SCE) [122–124].

Figure 24. Schematic presentation of a voltammogram of a M 1,2-DT (a) and a voltammogram of a TTF derivative, for comparison (b) [16,79].



In the literature, it can be found that there are a wide variety of redox values obtained from M 1,2-DTs under different conditions and electrochemical techniques. To help compare studies employing different reference electrode-couples, the redox potential values are converted *versus* a common reference electrode, the saturated calomel electrode (SCE), which is approximately equivalent to the Ag/AgCl electrode, according to the following relationship [19]: Ag/AgCl (in satur. KCl solution) = SCE (in satur. KCl solution) + 0.045 = Fc/Fc⁺ (in 0.2 M LiClO₄/MeCN) + 0.352 = Ag/Ag⁺ + 0.604 = NHE – 0.196 (V).

The conversion factors depend on the solvent and the supporting electrolyte [19,42,77]. Tables 5–8 give the $E_{1/2}(2-/1-)$, $E_{1/2}(1-/0)$ and $E(0/x+)$ (in V *versus* Ag/AgCl) as well as other electrochemical and OA data observed at room temperature from a number of selected M 1,2-DTs and selenium analogues. The difference $E(0/x+) - E_{1/2}(1-/0) \approx E_{\text{onset}}^{\text{ox}} - E_{\text{onset}}^{\text{rd}} = \Delta E$ is a measure of the electronic energy gap of the materials in solutions or suspensions [45,46,63,64,77,79]. One can see that the results from electrochemical measurements (of solutions, $E_{\text{g}}^{\text{elc}}$) are in agreement with the optical absorption $E_{\text{onset}}^{\text{opt}}$ of solutions in CS₂, while there is a large deviation from the data in the solid state (OA_{max} and $E_{\text{onset}}^{\text{opt}}$ of deposits or pellets), as well as from the electrical measurements (E_{g}^{el}) (see below). This is a consequence of the variety of intermolecular interactions arising from the S–S contacts, in the solid state. Namely, the difference is larger in cases of complexes with strong S–S interactions (Table 8). From these data, the HOMO and LUMO energy levels could be calculated via the following equations (see [47–50,63,64,79] and references therein).

$$E_{\text{HOMO}} = -(4.4 + E_{\text{onset}}^{\text{ox}}) \quad (3)$$

$$E_{\text{LUMO}} = -(4.4 + E_{\text{onset}}^{\text{rd}}) \quad (4)$$

Table 5. Redox potentials (V) and (solid state) OA_{max} (eV) of complexes * [14,64,77].

Complex	$E_{1/2}$ (2 ⁻ /1 ⁻)	$E_{1/2}$ (1 ⁻ /0)	E (0/x ⁺)	OA_{max}
[Ni(dmedt) ₂]	-1.070	-0.229	1.079	1.28
[Ni(tmedt) ₂]	-0.910	-0.140	1.050	1.24
[Ni(tmedt)(dddtt)]	-0.827	-0.099	0.964	1.21
[Ni(dpedit) ₂]	-0.864	-0.063	1.012	1.38
[Ni(dddtt) ₂]	-0.744	-0.058	0.875	1.04
[Ni(dpedit)(dddtt)]	-0.794 (-0.804)	-0.039 (-0.060)	0.988 (0.943)	1.17
[Ni(dmedt)(dmit)]	(-0.651)	(+0.039)	(1.207)	1.31
[Ni(tmedt)(dmit)]	-0.571	+0.064	1.197	1.28
[Ni(dpedit)(dmit)]	-0.559 (-0.544)	+0.167 (+0.102)	1.187 (1.173)	1.21
[Ni(dpedit)(dmio)]	-0.532	+0.170	1.185	1.38
[Ni(dddtt)(dmit)]	(-0.488)	(+0.210)	(1.105)	1.02
[Ni(dmit) ₂]	-0.232	+0.268	1.335	0.92
[Ni(dmio) ₂]	-0.200	+0.297	1.358	
[Ni(edo) ₂]	-0.75	-0.26	0.71	
[Ni(mnt) ₂]	-0.10	-0.81		
[Ni(Pr ₂ pipdt)(dmit)]	-1.165	-0.593	0.590	
[Ni(Me ₂ pipdt)(mnt)]	-0.963	-0.527	0.908	
[Ni(Pr ₂ tipdt)(mnt)]	-0.307	0.354	1.160	

* Observed vs. Ag/AgCl electrode. Calculated values from the equation $E_{1/2}(AB) = [E_{1/2}(AA) + E_{1/2}(BB)]/2$ are given in parentheses (where AA and BB are the symmetrical and AB the corresponding unsymmetrical complexes); $0 < x \leq 1$; E (0/x⁺) usually is irreversible wave; OA_{max} in solid state.

Table 6. Electrochemical * and (solid state) OA ** data of selected complexes [64,77].

Complex	E_{onset}^{rd} (V)	E_{onset}^{ox} (V)	E_{onset}^{op} (eV)	E_{LUMO} (eV)	E_{HOMO} (eV)
[Ni(dmedt) ₂]	-0.145	0.958	1.18 [1.10]	-4.25	-5.36
[Ni(tmedt) ₂]	-0.135	0.905	0.90 [1.03]	-4.26	-5.30
[Ni(tmedt)(dddtt)]	-0.042	0.837	0.88 [0.88]	-4.36	-5.24
[Ni(dpedit) ₂]	0.000	0.860	0.95 [0.86]	-4.40	-5.26
[Ni(dddtt) ₂]	+0.052	0.770	0.76 [0.72]	-4.45	-5.17
[Ni(dpedit)(dddtt)]	+0.100	0.833	0.82 [0.73]	-4.50	-5.23
[Ni(dmedt)(dmit)]	(+0.122)	(1.024)	0.91 [0.90]	(-4.52)	(-5.42)
[Ni(tmedt)(dmit)]	+0.142	0.997	0.95 [0.86]	-4.54	-5.39
[Ni(dddtt)(dmit)]	(+0.221)	(0.930)	0.80 [0.71]	(-4.62)	(-5.33)
[Ni(dpedit)(dmit)]	+0.270	1.020	0.85 [0.75]	-4.67	-5.42
[Ni(dpedit)(dmio)]	+0.280	1.017	0.92 [0.74]	-4.68	-5.42
[Ni(dmit) ₂]	+0.390	1.090	1.0 [0.70]	-4.79	-5.48
[Ni(dmio) ₂]	+0.450	1.130	1.1 [0.68]	-4.85	-5.53

* Observed vs. Ag/AgCl. Calculated values from equation $E_{onset}(AB) = [E_{onset}(AA) + E_{onset}(BB)]/2$ as well as the corresponding E_{LUMO} and E_{HOMO} values are given in parentheses; ** E_{onset}^{op} observed from thin deposits. Calculated E_{onset}^{op} values ($=E_g^{elc}$) from electrochemical data ($E_{onset}^{ox} - E_{onset}^{rd}$) 1 eV, considering $x = 1$, are given in brackets.

Table 7. Calculated E_{LUMO} and E_{HOMO} values and the corresponding electrochemical and optical absorption data [63,79].

Complex	$E_{1/2}(1-/0)$ (V)	$E_{\text{onset}}^{\text{rd}}$ (V)	$E_{\text{onset}}^{\text{ox}}$ (V)	$E_{\text{onset}}^{\text{opt}}$ (eV)	E_{LUMO}^* (eV)	E_{HOMO}^* (eV)
[Ni(dpdt)(pddt)]	+0.036	+0.155	+0.884	0.88	-4.55	-5.28 [-5.43]
[Ni(dpdt)(dddt)]	-0.039	+0.100	+0.833	0.82	-4.51	-5.23 [-5.33]
[Pd(dpdt)(dddt)]	+0.030	+0.161	+0.797	0.92	-4.56	-5.20 [-5.48]
[Pt(dpdt)(dddt)]	+0.055	+0.070	+0.900	0.95	-4.47	-5.30 [-5.42]
[Ni(dpdt)(dmit)]	+0.167	+0.270	+1.020	0.85	-4.67	-5.42 [-5.52]
[Pd(dpdt)(dmit)]	+0.230	+0.250	+0.920	0.96	-4.65	-5.32 [-5.41]
[Au(dpdt)(dddt)]	+0.300	+0.350	0.850	0.65	-4.75	-5.25 [-5.40]
[Au(dpdt) ₂]	+0.315	+0.403	0.852	0.61	-4.83	-5.22 [-5.44]

* The E_{LUMO} values were calculated from the reduction onset values ($-E_{\text{LUMO}} = 4.4 + E_{\text{onset}}^{\text{rd}}$). The E_{HOMO} values were calculated from the oxidation onset values ($-E_{\text{HOMO}} = 4.4 + E_{\text{onset}}^{\text{ox}}$). Also, E_{HOMO} values calculated from electrochemical and OA data ($E_{\text{HOMO}} = E_{\text{LUMO}} - E_{\text{onset}}^{\text{opt}}$) are given in brackets.

Table 8. Electrochemical, optical and electrical data for selected M 1,2-DTs [48–50,77].

Complex	$E_{1/2}(1-/0)$	$E(0/x+)$	$E_{\text{g}}^{\text{elc}}$	OA_{max}	$E_{\text{onset}}^{\text{opt}}$	E_{g}^{el}
[Ni(dmdt) ₂]	-0.14	0.74	0.88	4545	0.25 [1.0]	0
[Ni(tmdt) ₂]	-0.12	0.80	0.92	4545	0.25 [1.0]	0
[Ni(dt) ₂]	0.01					0.070
[Pd(dt) ₂]				1289	0.2 [1.0]	
[Ni(ptdt) ₂]	-0.04	1.39	1.35	2127	0.55 [1.0]	0.060
[Ni(etdt) ₂]	-0.05			1417	0.50 [1.1]	
[Ni(dmdt)(dmio)]	(0.08)			1270	0.60 [1.0]	
[Ni(dmdt)(dmit)]					0.72 [1.0]	
[Ni(dmstfdt)(dmio)]				1212	0.83 [1.2]	
[Ni(dt)(dmit)]	(0.14)			1245	0.73 [1.03]	
[Ni(pddt)(dmio)]					0.80 [1.2]	0.26, 0.36
[Ni(dmeds)(dmit)]					1.03 [1.13]	0.38, 0.36

Electrochemical data: $E_{1/2}(1-/0)$, $E(0/x+)$ and $E_{\text{g}}^{\text{elc}} \approx E(0/x+) - E_{1/2}(1-/0)$ (V, versus Ag/AgCl electrode); OA_{max} position of a thick deposit (polycrystalline samples) (nm); $E_{\text{onset}}^{\text{opt}}$ of the OA band in solid state (deposits or pellets) (eV); the corresponding onset from solutions in CS₂ are given in brackets and the energy gap from electrical measurements, E_{g}^{el} (eV).

These are applied when the $E_{\text{onset}}^{\text{ox}}$ and $E_{\text{onset}}^{\text{rd}}$ are given versus Ag/AgCl as reference electrode. If one of the E_{onset} is observed by CV, this value and the difference $E_{\text{onset}}^{\text{ox}} - E_{\text{onset}}^{\text{rd}} \approx E_{\text{onset}}^{\text{op}}$ obtained from the OA spectra of solutions, suspensions or very thin films could be used for the calculation of HOMO and LUMO energy values. However, HOMO energy values could be estimated from ultraviolet photoelectron spectra and the LUMO energy values from the inverse photoelectron spectra, in the solid state [125]. The electrochemical parameters of unsymmetrical M 1,2-DTs (AB) occur in between those of the corresponding symmetrical (AA, BB) as in the case of the OA parameters. If the couples are reversible, the redox values obey the following equation as in the case of TTFs [16].

$$E_{(\text{AB})} = [E_{(\text{AA})} + E_{(\text{BB})}]/2 \quad (5)$$

The calculated values of several unsymmetrical complexes are given in Tables 5–8 in comparison to the observed ones. It can be seen that the values of LUMO and HOMO levels vary from *ca.* 4.25 to 4.85 and from *ca.* 5.17 to 5.68 eV, respectively. It has been demonstrated that these compounds are stable in air ($\text{H}_2\text{O} + \text{O}_2$), because the LUMO value is larger than 4 eV (see [47] and references therein). This finding is almost equivalent with the suggestion that the species (such as neutral M 1,2-DTs) with $E_{1/2} < 0.00$ V (*vs.* SCE) are susceptible to air oxidation in solution ($\text{H}_2\text{O} + \text{O}_2$), while species with $E_{1/2} > 0.00$ V are stable in air. A number of neutral M 1,2-DTs were prepared by oxidation of the corresponding anionic complexes. In these reactions and others similarly involving oxidation, proper selection of the oxidizing agent is crucial. However, the knowledge of the redox values of the species could be a guide to the synthesis of new compounds [14,15,48–50,64,77]. For example, if the species has $E_{1/2} < 0.2$ V the oxidation can be obtained with I_2 , otherwise, a stronger oxidant should be used [19]. Also, if a monoanionic M 1,2-DT has two reversible redox processes between the dianions and neutral complexes at *ca.* -0.7 and 0 V (*vs.* Ag/AgCl) as in $[\text{Ni}(\text{dddt})_2]$ further oxidation is associated with the formation of partially oxidized compounds $\{\text{M } 1,2\text{DT}\}^{x+}$. If these values are -0.23 and 0.26 V, as in $[\text{Ni}(\text{dmit})_2]$, the oxidation gives cation deficient salts such as $[\text{Ni}(\text{dmit})_2]^{x-}$. In the cases of complexes with extended TTF dithioleto ligands these values are *ca.* -0.4 and 0 V, respectively, the oxidation gives neutral complexes. In other words, the knowledge of redox values is a guide for fabrication of several stable (in air) electronic and optoelectronic devices (see below).

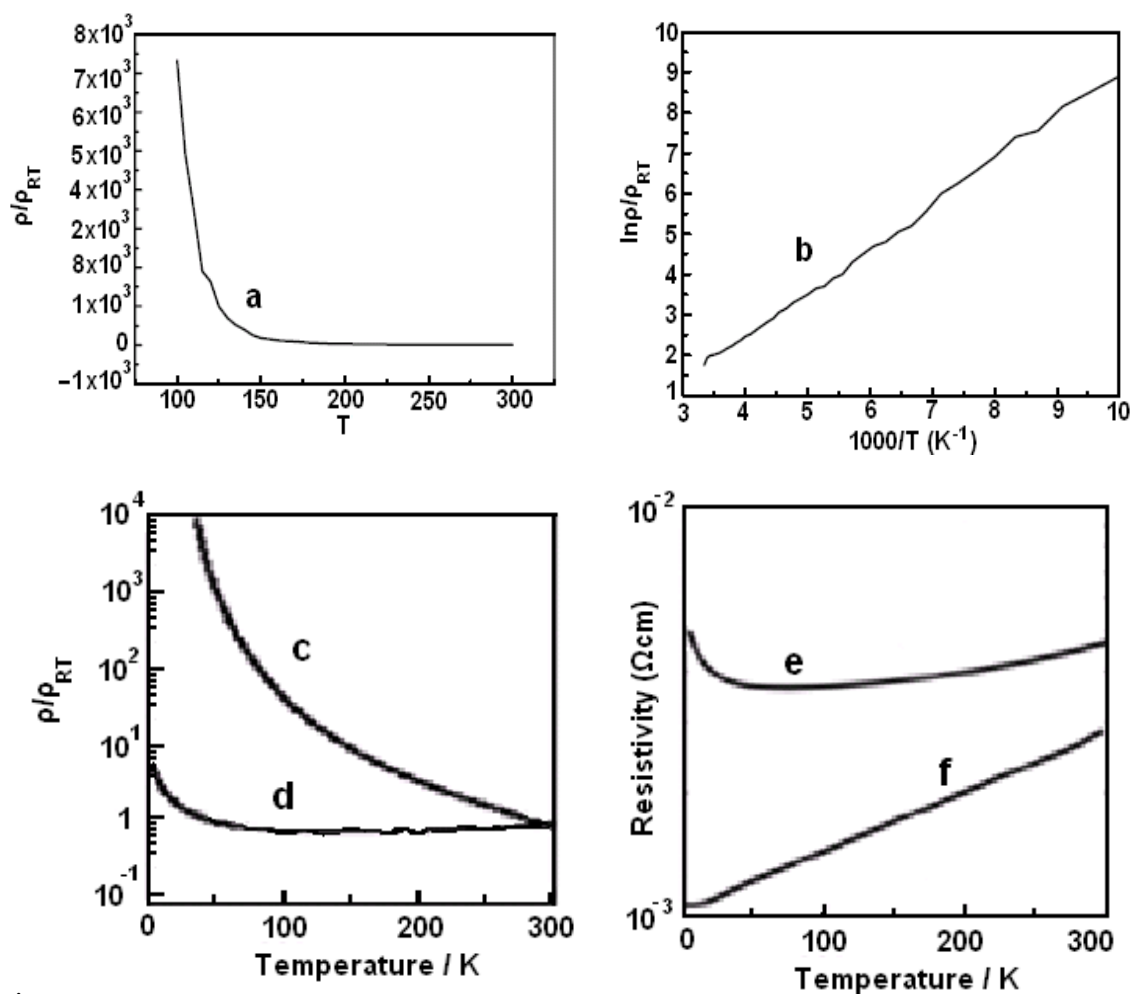
6. Electrical Properties

As in other cases of organic and inorganic materials, one may classify M 1,2-DTs as metals with room temperature conductivity $\sigma_{\text{PT}} \geq 10^2 \text{ Scm}^{-1}$, semiconductors with $10^2 \geq \sigma_{\text{RT}} \geq 10^{-10} \text{ Scm}^{-1}$, and insulators with $\sigma_{\text{PT}} \leq 10^{-10} \text{ Scm}^{-1}$ [20–27,51]. Monoanionic M 1,2-DTs are weak semiconductors or insulators; cationic are metallic or semiconducting materials, while cation deficient and neutral could be semiconducting or metallic. Some cation deficient complexes are superconducting materials [20–27]. From the neutral (*i.e.*, single component) M 1,2-DTs, some symmetrical, usually with extended TTF-dithiolato ligands, were found to be metallic without the need to form charge transfer salts ([22,26,35] and references therein). It has been considered that, unlike conventional organic conductors (*i.e.*, those based on TTFs) consisting of π -conduction layers and insulating anionic layers, the single compound molecular conductors (*i.e.*, M 1,2-DTs) tend to have 3D stable metallic bands [43]. Here, the results obtained mainly from neutral symmetrical and unsymmetrical complexes, based on some ligands of Tables 1–3, with semiconducting behavior, as well as those obtained from some anionic complexes for comparison are primarily discussed. The electrical characteristics of some neutral complexes are tabulated in Table 9 with the corresponding structural and optical ones, for comparison. In the cases of monoanionic complexes, such as $(\text{Bu}_4\text{N})[\text{Ni}(\text{dmit})_2]$ and $(\text{Bu}_4\text{N})[\text{Ni}(\text{dddt})_2]$, the conductivity at room temperature has values 10^{-8} and $5 \times 10^{-5} \text{ S/cm}$, respectively. However in cation deficient compounds of the type $(\text{Bu}_4\text{N})_x[\text{Ni}(\text{dmit})_2]$ the room temperature conductivity varies from 10^{-3} to 10 S/cm as x increases from 0.25 to 0.29 (see [20] and ref. 102 cited therein). Figure 25 shows the resistivity *versus* the temperature and *versus* the inverse temperature for a polycrystalline pellet of $(\text{Bu}_4\text{N})_{0.25}[\text{Ni}(\text{dmit})_2]$ (see [9] and ref. 20 cited therein, [54] and ref. 6 cited therein, [69] and ref. 26 cited therein).

Table 9. Structural, optical and electrical characteristics of some neutral M 1,2-DTs [15,23,29,36,43,45,46,57,77,90].

Complex	Space Group	S-S (Å)	OA _{max} (nm, CS ₂)	OA _{max} (nm, Sol. St)	σ _{RT} (Scm ⁻¹)	E _a (meV)
α-[Ni(dpedit) ₂]	P2 _{1/n}		875			
β-[Ni(dpedit) ₂]	Pī		875			
[Ni(ddd) ₂]	P2 _{1/a}	<3.70	1033	>1119		
[Ni(dmit) ₂]	>>	<3.70, 3.58	1030	1017	Sem. 3.5 × 10 ⁻³	
[Ni(etodd) ₂]	Pī	<3.70				
[Ni(tmedit)(ddd)]	P2 _{1/c}	3.59	936	1030		
[Ni(tmedit)(dmit)]	>>	3.70–3.73	945	1037		
[Ni(pddt)(dmio)]	>>	3.49, 3.56	978	935	Sem. 2.5 × 10 ⁻⁵ , 1 × 10 ⁻⁹	130, 180
[Ni(dmeds)(dmit)]	Pī	3.59	950	920	Sem. 1.5 × 10 ⁻⁵ , 2.5 × 10 ⁻⁸	190, 180
[Ni(dpedit)(ddd)]	Pbc2 ₁	3.76	955	1059		
[Ni(dpedit)(pddt)]	>>	3.746	947	981		
[Au(dpedit) ₂]	Pī	4.5	1480	1480		
[Au(ddd) ₂]	P2 _{1/n}	3.59–3.67	1960		Sem. 1 × 10 ⁻⁴	
[Au(bdt) ₂]	>>	3.60–3.66		2062	Sem. 0.11	
[Ni(dmdt) ₂]	Pī		978	4595	300–400 Met > 230 K	
[Pd(dmdt) ₂]					Sem. 150	
[Ni(tmtdt) ₂]	Pī	3.44–3.75	1005	4595	300–400 Met > 0.6 K	
[Co(dmdt) ₂]					Sem. 0.05	85
[Co(tmtdt) ₂]					Sem. 1.5	24
[Cu(dmdt) ₂]		<3.7			Sem. 3.0	40
[Cu(tmtdt) ₂]					Sem. 5.1	63
[Au(dmdt) ₂]					Sem. 12	9 (300–50 K)
[Au(tmtdt) ₂]	Pī	3.43–3.64			Sem. 15	20 (300–50 K)
[Ni(dt) ₂]					Sem. 16	35
[Pd(dt) ₂]	P2 _{1/m}	<3.7		1282	Sem. 0.3	94
[Co(dt) ₂]					Met. 19	
[Ni(etdt) ₂]					Sem. 10 ⁻⁴	
[Ni(eodt) ₂]					8 Met > 120K	
[Ni(chdt) ₂]					Sem. 2.0	38
[Ni(hfdt) ₂]					Sem. 1.4 × 10 ⁻⁴	22
[Au(hfdt) ₂]					Sem. 3.2 × 10 ⁻⁴	220
[Ni(ptdt) ₂]	C2/m	3.37		2127	Sem. 7	30
[Pt(tmtdt) ₂]					350 Met > 4 K	
[Ni(tmstdt) ₂]					100 Met > 100 K	
[Ni(dtdt) ₂]					2.5–200	
[Au(dtdt) ₂]					8	
[Ni(a-tdt) ₂]					2.5–24	
[Au(a-tdt) ₂]					5	
[Au(ptdt) ₂]		3.26			2	

Figure 25. Resistivity *versus* the temperature (**a,c,d,e,f**) and *versus* the inverse temperature (**b**) for polycrystalline pellets of $(\text{Bu}_4\text{N})_{0.25}[\text{Ni}(\text{dmit})_2]$ (**a,b**) [77], $[\text{Ni}(\text{chdt})_2]$ (**c**), $[\text{Ni}(\text{eodt})_2]$ (**d**) and $[\text{Ni}(\text{tmdt})_2]$ (**e**) as well as in a single crystal of $[\text{Ni}(\text{tmdt})_2]$ (**f**). Panel c and d was reproduced from [22] and panel e and f from [23] with permissions of the American Chemical Society.



From the slopes of the plots the activation energy (E_a) and/or the energy gap (E_g), values could be

$$\frac{1}{\sigma(T)} = \rho(T) = \rho_0 \exp\left(\frac{E_a}{kT}\right) \quad (6)$$

calculated via the Arrhenius equation where ρ_0 is a temperature independent constant, k is the Boltzman constant and $E_a = E_g/2$. For the cation deficient compound $(\text{Bu}_4\text{N})_{0.25}[\text{Ni}(\text{dmit})_2]$ the activation energy at low temperatures was found, via this equation, to be 84 meV [77]. Cation deficient complexes based on dmit with several cations, metals and compositions (x) were found to be semiconductors, conductors and superconductors (see [20,69]). Some neutral M 1,2-DTs and TTFs exhibit similar behavior (see [15,21,77]). Single crystals of the neutral $[\text{Ni}(\text{dmit})_2]$ exhibit semiconducting behavior with $\sigma_{\text{RT}} = 3.5 \times 10^{-3}$ S/cm [69]. Figure 25 shows ρ vs. T of polycrystalline pellets of $[\text{Ni}(\text{chdt})_2]$ and $[\text{Ni}(\text{eodt})_2]$ [22] as well as, ρ vs. T of a polycrystalline pellet and a single crystal of $[\text{Ni}(\text{tmdt})_2]$ [23]. The change in behavior (from metallic to semiconducting) is due to

the decreasing intermolecular contacts as was observed in the optical absorption spectra (Figures 21 and 22). Figure 26 shows the plots of ρ vs. $1/T$, obtained from a single crystal of $[\text{Ni}(\text{pddt})(\text{dmio})]$ [36] of which the crystal structure has already been discussed above. It was found that the room temperature conductivity is $\sigma_{\text{RT}}(\parallel) = 2.5 \times 10^{-5} \text{ Scm}^{-1}$ and $\sigma_{\text{RT}}(\perp) = 1 \times 10^{-9} \text{ Scm}^{-1}$. This means that there is anisotropy of 2.5×10^4 . From Equation 6, one can find $E_a(\parallel) = 0.13$, and $E_a(\perp) = 0.18 \text{ eV}$ [35].

Figure 26. Plots of resistivity *versus* the inverse temperature for a single crystal of $[\text{Ni}(\text{pddt})(\text{dmio})]$ with current approximately parallel (\parallel) and perpendicular (\perp) to the ab -plane. Reproduced from [36] by permission of the Verlag der Zeitschrift für Naturforschung.

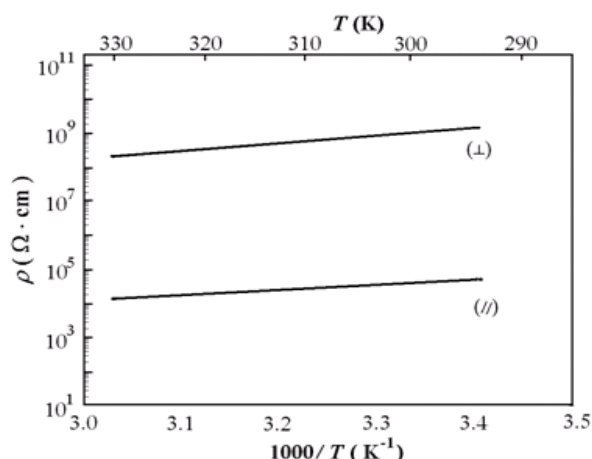
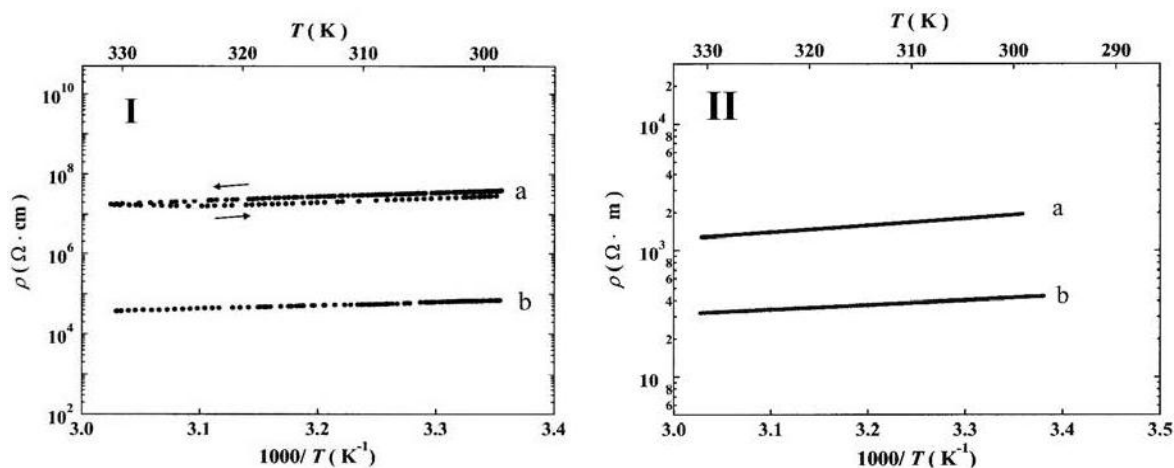


Figure 27 shows the resistivity *versus* the inverse temperature for a single crystal of $[\text{Ni}(\text{dmeds})(\text{dmit})]$ with currents approximately parallel (a) and perpendicular (b) to the ab plane [50]. In this case $\sigma_{\text{RT}}(\parallel) = 1.5 \times 10^{-5} \text{ Scm}^{-1}$, $\sigma_{\text{RT}}(\perp) = 2.5 \times 10^{-8} \text{ Scm}^{-1}$, $\sigma_{\text{RT}}(\parallel)/\sigma_{\text{RT}}(\perp) = 6 \times 10^2$, $E_a(\parallel) = 0.19$, and $E_a(\perp) = 0.18 \text{ eV}$ [50], for the current parallel (\parallel) and perpendicular (\perp) to the ab -plane. It has been found that after a series of heating/cooling cycles the resistivity decreases [50].

Figure 27. Plots of resistivity *versus* the inverse temperature for a single crystal of $[\text{Ni}(\text{dmeds})(\text{dmit})]$ with current approximately parallel (\parallel) and perpendicular (\perp) to the ab -plane, before (I) and after (II) applying a number of heating/cooling cycles. Reproduced from [36] by permission of the Verlag der Zeitschrift für Naturforschung.



Conductivity measurements on compressed pellets of [Ni(dmcds)(dmit)], [Ni(dmedt)(dmit)] and [Ni(dpedit)(dsit)] gave $\sigma_{RT}(\text{pellet}) = 1 \times 10^{-6}$, 1.2×10^{-7} , and $1 \times 10^{-7} - 5 \times 10^{-6} \text{ Scm}^{-1}$, respectively. The $E_g(\text{pellet})$ values were found to be 0.45, 0.50–0.80 and 0.46 eV, respectively. The σ_{RT} values of [Ni(dpedit)(dmit)] and [Ni(dcdt)(dmit)] were found to be very small ($<10^{-9} \text{ Scm}^{-1}$) [35,50,58]. Measurements on a single crystal of [Au(bdt)₂] showed, $\sigma_{RT}(\parallel) = 0.11 \text{ Scm}^{-1}$ and $E_a(\parallel) = 0.3 \text{ eV}$ [29]. From structural, optical and electrical data from single crystals or polycrystalline samples, reported above and/or summarized in Tables 4 and 9, it can be expected that the energy gap values of each sample (or crystallographic directions) obey Equation 2. This means that, as the interactions increase, the E_g decreases, the optical absorptions bands are red shifted and the material, because of Equation 6, becomes more conducting (see also [32,134]). Calculations of t_1 and t_2 from crystallographic data are needed for a comparison with the experimental data. The conductivity measurements on some M 1,2-DTs after illumination with visible-near IR light exhibit a broad band close to that of the OA band [24,59,62]. These materials can be used as photodetectors [24,59,62].

Recently, the results of electrical measurements on M 1,2-DTs under the conditions of field effect transistor (FET) have been reported [37,39,47,56,57,65,93,113]. These results are discussed here and compared with those obtained from donors (e.g., TTFs) or acceptors (e.g., TCNQ) [51,66,126]. Mainly, electrical circuits like those shown in Figure 8 suitable for measurements on thin deposits or single crystals of M 1,2-DTs have been used. The observed currents are due to the semiconductor-insulator interface which is a thin (2-dimensional) layer in the semiconductor size, the channel of the semiconductor; the rest of the material is inert and does not contribute drastically to this kind of current. As an example, the process of measurement on [Ni(dpedit)(dmit)] thin film is described [47]. Si wafers of (p-type) as a gate electrode, with 200 nm SiO₂ layer at the gate electrode, gold source and drain electrodes were defined in a two terminal bottom contact configuration (Figure 8a), with channel width (W) of 10 mm and length (L) of 10 μm . A 10 nm titanium was used as an adhesion interlayer for the gold on SiO₂. The SiO₂ was treated with the primar hexamethyldisilazane prior to semiconductor deposition, in order to passivate its surface. Films of [Ni(dpedit)(dmit)] were then drop cast on top from a solution in CH₂Cl₂. Under appropriate biasing conditions strong hole and electron accumulation has been observed. In particular, for negative drain (V_D) and gate (V_G) voltages, accumulation of holes is evident, while for positive V_D and V_G , electron accumulation has been observed. Figure 28a shows the output current-voltage characteristics and Figure 28b shows the transfer characteristics at various drain voltages on a channel of [Ni(dpedit)(dmit)] [47]. From the curves and the Equations 7 and 8, the hole and electron field effect mobilities (μ_h , μ_e) have been calculated.

$$\text{For linear regime } \mu_{lin} = \frac{L}{W} \frac{1}{C_i V_D} \frac{\partial I_D}{\partial V_G} \quad (7)$$

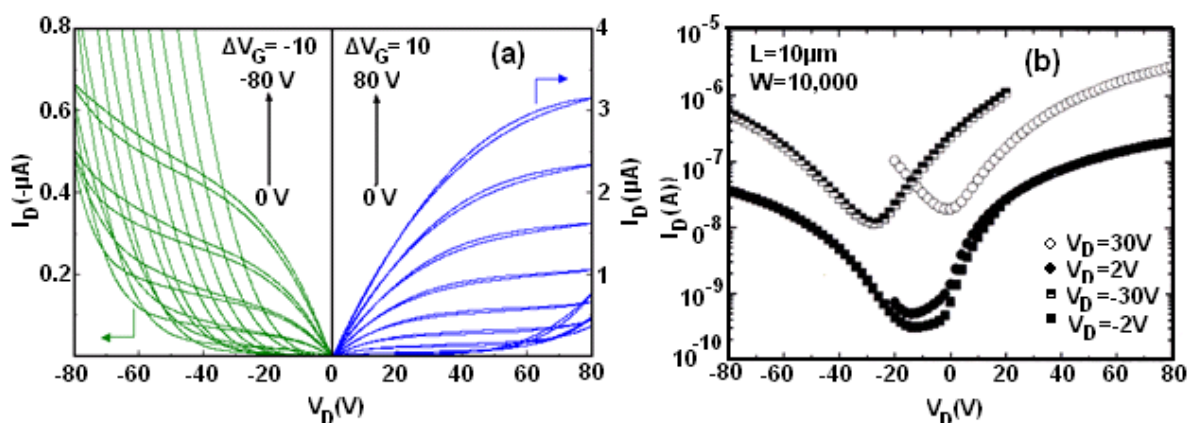
$$\text{For the saturated regime } \mu_{sat} = \frac{L}{W} \frac{1}{C_i} \frac{\partial^2 I_D}{\partial V_G^2} \quad (8)$$

Where C_i is the capacitance per unit area of the insulator layer (given by $C_i = \epsilon\epsilon_0/d$, with d the thickness of the layer, ϵ is the dielectric constant of the insulator and ϵ_0 the permittivity in vacuum).

From the calculations the maximum hole and electron mobilities have been found to be 1×10^{-4} and $3 \times 10^{-4} \text{ cm}^2/\text{Vs}$, respectively. The on-off current ratio was calculated from the data of the transfer characteristics and Equation 9 assuming that the semiconductor film of thickness t has a uniform (bulk) conductivity, σ , and uniform mobility, μ , the ratio is of the order $10^2 - 10^3$.

$$\frac{I_{on}}{I_{off}} = 1 + C_i V_D \frac{\mu}{2\sigma t} \quad (9)$$

Figure 28. Output current-voltage characteristics (a) and transfer characteristics at various drain voltages (b) obtained from an ambipolar channel based on [Ni(dpdt)(dmit)]. Reproduced with permission from [47] by permission of the American Institute of Physics.



Measurements on $(\text{NO})_x[\text{Ni}(\text{dmit})_2]$ ($1 > x \geq 0$) films showed that the behaviour is of n-type in any x value [25]. When $x = 1$ (monoanionic) the mobility (μ_e) is small 2.4×10^{-5} , as in most cases of M 1,2-DTs. However after doping [25] (oxidation) with iodine, the material became cation deficient ($1 > x > 0$) or neutral ($x = 0$) as was discussed above for $(\text{Bu}_4\text{N})_x[\text{Ni}(\text{dmit})_2]$ (see [6]). In this last case ($1 > x > 0$) the mobility in a FET device found a much larger $\mu_e = 0.18 \text{ cm}^2/\text{Vs}$ [25]. The results of measurements from the reported M 1,2-DTs are summarized in Table 10. Similar measurements have been made also on single crystals of M 1,2-DTs with electrical circuit connections as those of Figure 8b (see [77,79,105,135–139] and references therein). Figure 29 shows a photograph of a single crystal of [Ni(tmtdt)(ddd)] with S-D electrodes of TTF-TCNQ ($L = W = 100 \mu\text{m}$), perylene film as insulator, and Au-paste as gate electrodes [105].

Table 10. LUMO, HOMO values (eV), mobilities (cm^2/Vs), I_{on}/I_{off} and σ_{RT} (S/cm).

Complex	L	H	μ_e	μ_h	I_{on}/I_{off}	σ_{RT}	Ref.
[Ni(L11a) ₂]	0.83 (H-L)		ca. 10^{-6}	ca. 10^{-7}		5×10^{-11}	[113]
[Ni(L11b) ₂]	0.87 (H-L)		ca. 10^{-2}	ca. 10^{-7}			[113]
[Ni(L11b) ₂]			ca. 10^{-8}	ca. 10^{-8}		5×10^{-11} (p)	[93]
[Ni(L12a) ₂]						2.5×10^{-5} (c)	[93]
[Ni(L9a) ₂]	4.4–4.6 (L)		2.0×10^{-5} (v)	3×10^{-6} (air)	(Al)	10^2 (air), (v)	[56]
[Ni(L9b) ₂]	4.4–4.6 (L)		1.3×10^{-5} (v)		(Al)	2×10^2 (v)	[56]
[Ni(L9b) ₂]	4.4–4.6 (L)		1.3×10^{-4} (v)		(TTF-TCNQ)	2×10^2 (v)	[56]
[Ni(L9c) ₂]	4.4–4.6 (L)		6.8×10^{-5} (v)		(TTF-TCNQ)	10^4 (v)	[56]
[Ni(L9d) ₂]	4.4–4.6 (L)		5.0×10^{-5} (v)	9×10^{-5} (air)	(TTF-TCNQ)	30 (v), 20 (air)	[56]
[Ni(L9e) ₂]	4.4–4.6 (L)		6.4×10^{-6} (v)	6.6×10^{-5} (air)	(TTF-TCNQ)	10 (v), 16 (air)	[56]
[Ni(L15c) ₂]	4.1	5.6	1.3×10^{-3} (2.8)				[57]
[Ni(L8d) ₂]	4.1	5.8	2.5×10^{-3}				[57]
[Ni(L8a) ₂]	4.1	5.8	4.5×10^{-5}				[57]

Table 10. Cont.

[Ni(dpedit) ₂]	4.36		$3 \times 10^{-6} - 2 \times 10^{-5}$ (v)		10^2 (v)		[39]
[Ni(L10a) ₂]	4.3	5.2	2.5×10^{-4}	2×10^{-5}			[37,38]
[Ni(dpedit)(dmit)]	4.43	5.28	3×10^{-4}	1×10^{-4}	10^3	10^{-9} (p)	[47]
[Ni(tmedt)(dddt)]	4.36	5.24	0.02–0.045 (c)	0.02 (c)	1.4 (c)		[77,79]
[Ni(dpedit)(dddt)]	4.50	5.23	$1 \times 10^{-4}, 3 \times 10^{-4}$ (c)	3×10^{-4} (c)	4 (c)		[77,79]
(NO)[Ni(dmit) ₂]			$2-4 \times 10^{-5}$				[25]
(NO) _x [Ni(dmit) ₂]			0.18				[25]

v = in vacuum; air = in O₂ + H₂O; c = single crystal; p = powder; L = LUMO, H = HOMO, NO = *N*-octadecylpyridinium; $1 > x \geq 0$.

Figure 29. Photograph of a single crystal of [Ni(tmedt)(dddt)] (No. 1) and electrodes [105].

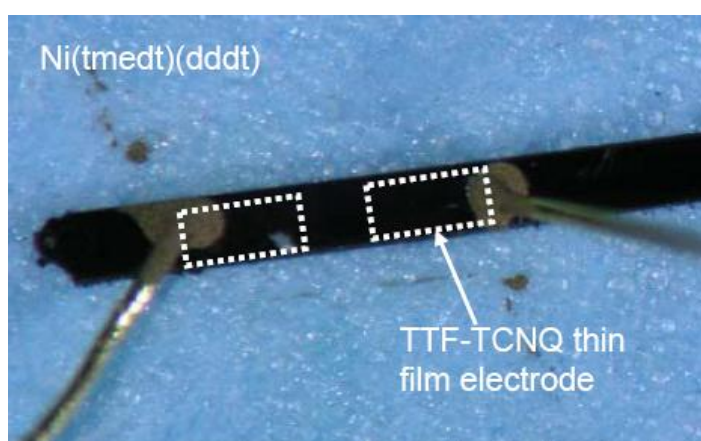


Figure 30 shows the obtained characteristics. In this case, the material (No. 1) behaves as an n-type semiconductor with a mobility of $0.02 \text{ cm}^2/\text{Vs}$ and $I_{\text{on}}/I_{\text{off}}$ of 1.4. On recrystallization of compounds the mobility values were increased. Figure 31 shows the obtained characteristics from a single crystal (No. 2) of recrystallized [Ni(tmedt)(dddt)] and from a single crystal of [Ni(dpedit)(dddt)]. It can be seen that, when TTF-TCNQ electrodes are used (work function = 4.6 eV) [135] the complex [Ni(tmedt)(dddt)] exhibits n-type behaviour with a mobility $\mu_e = 0.045 \text{ cm}^2/\text{Vs}$, while using Au electrodes (work function = 4.7 eV) the complex exhibits ambipolar behaviour with $\mu_e = \mu_h = 0.02 \text{ cm}^2/\text{Vs}$, because of the decreasing hole barrier (see below). Also the crystal of [Ni(dpedit)(dddt)] with TTF-TCNQ electrodes exhibits ambipolar behaviour (Figure 31) with mobility values $\mu_e = 1 \times 10^{-4}$ and $\mu_h = 3 \times 10^{-4} \text{ cm}^2/\text{Vs}$; and $I_{\text{on}}/I_{\text{off}}$ of 4. These low values of $I_{\text{on}}/I_{\text{off}}$ are attributed to small band gap values or to mid gap levels [65] of materials, in the solid state. The results on a single crystal are summarized in Table 10. However, experiments performed on crystals in other directions, *i.e.*, perpendicular to the needle axes of the crystals are needed. The results on single crystals of Ni 1,2-DTs are similar to those reported for organic single crystals with p-type behaviour [23,24], as well as with n-type behaviour [135,139].

Figure 30. Output current-voltage (a) and transfer (b) characteristics obtained from a single crystal of [Ni(tmedt)(dddt)] (No. 1) [77,105].

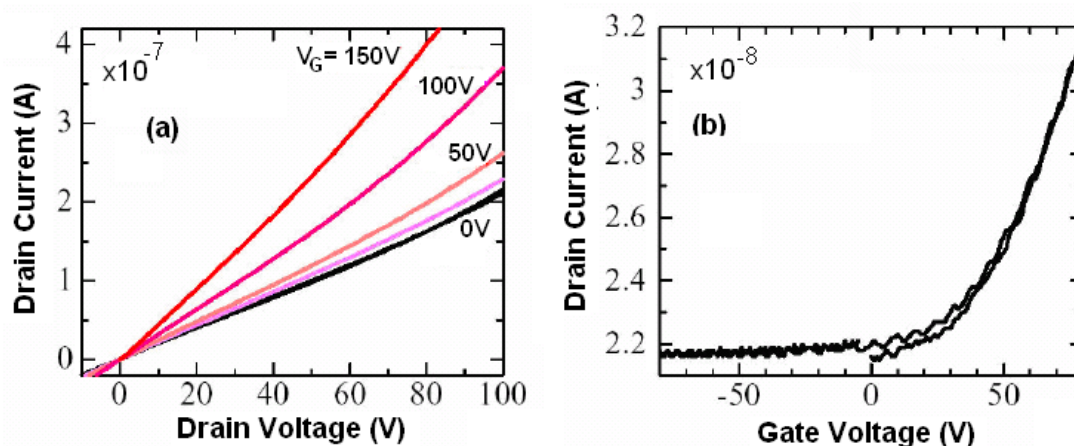
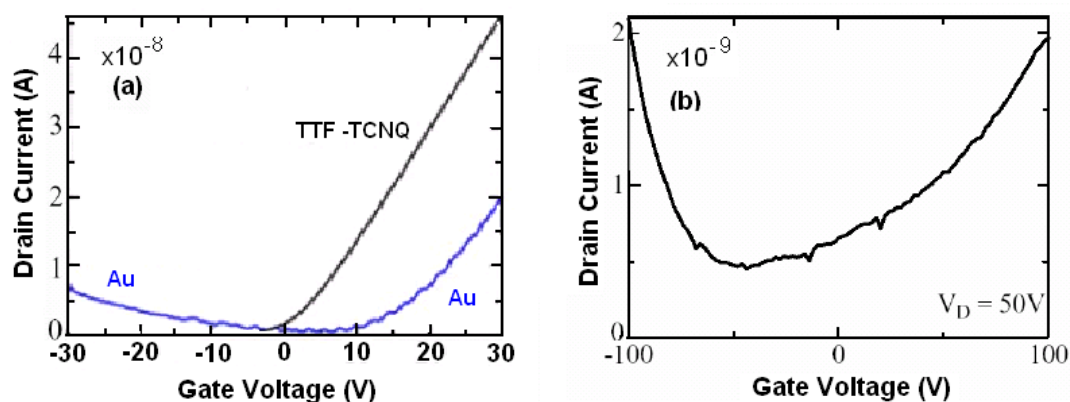


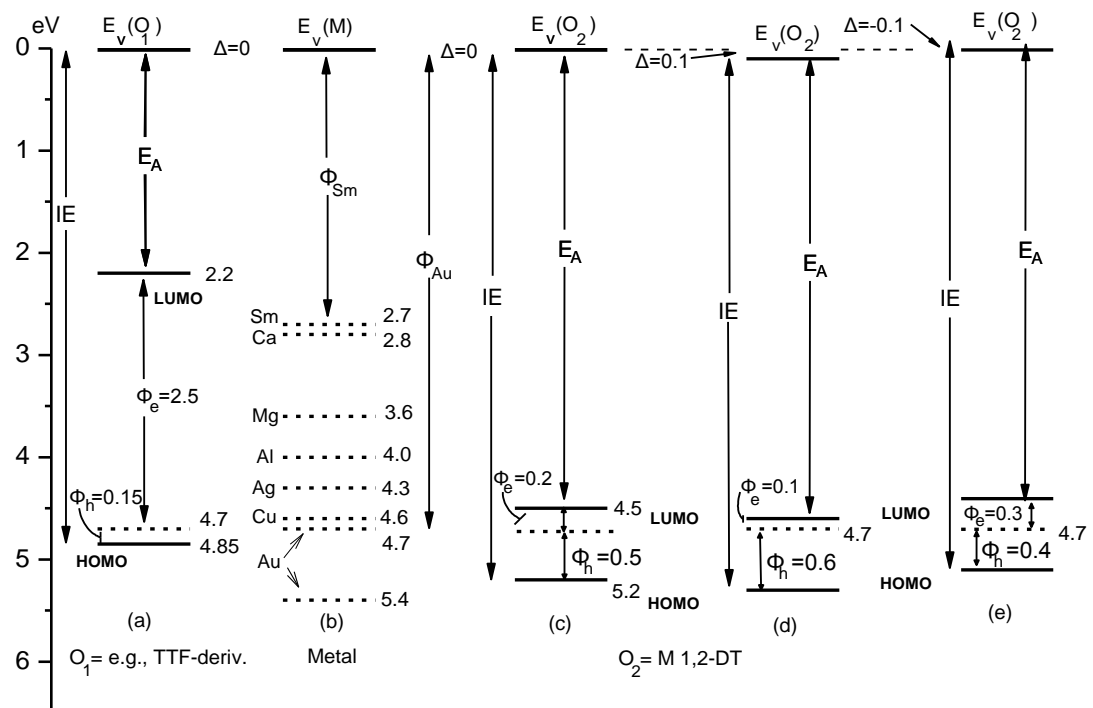
Figure 31. Transfer characteristics for a single crystal of (No. 2) [Ni(tmedt)(dddt)] (a) and for a single crystal of [Ni(dpedit)(dddt)] (b) [77,105].



From the data of Table 10 and the data obtained from other materials, e.g., TTFs [51,66,126,135–138], it can be said that a number of factors concerning the semiconductor component (e.g., S–S contacts, homoc resistance) and factors concerning other components of FETs (e.g., electrodes, insulator) influence the value of mobility and I_{on}/I_{off} of systems. The data obtained from [Ni(L15c)₂] ($\mu_e = 2.8 \text{ cm}^2/\text{Vs}$) [57], NO_x[Ni(dmit)₂] ($\mu_e = 0.18 \text{ cm}^2/\text{Vs}$) [25] and [Ni(tmedt)(dddt)] ($\mu_e = \mu_h = 0.02 \text{ cm}^2/\text{Vs}$) are close to those of porous Si. However, to obtain the optimum values of mobility and I_{on}/I_{off} , more experiments are needed, from M 1,2-DTs with several ligands, which could contribute positively or negatively to the interference barrier or to the LUMO or HOMO levels, *etc.*, in accordance with the diagram of Figure 32. It shows the characteristic energy levels of several components in a FET device, *i.e.*, the work function values of metal electrodes (Sm, Ca, Mg, Al, Cu and Au), e.g., $\Phi_{Au} = 4.7 \text{ eV}$ (O, C-contaminated) and $\Phi_{Au} = 5.4 \text{ eV}$ (clean) [125]; the electron affinity (LUMO) and ionization energy (HOMO) values of a donor (:TTF) molecule and an acceptor (:M 1,2-DT) molecule and the resulting, electron injection and hole injection barriers (Φ_e , Φ_h) of the system considering several values of the interface dipole (Δ).

These kind of diagrams could be useful guides for selection of appropriate components in order to obtain an optimum value of the mobility in FET circuits.

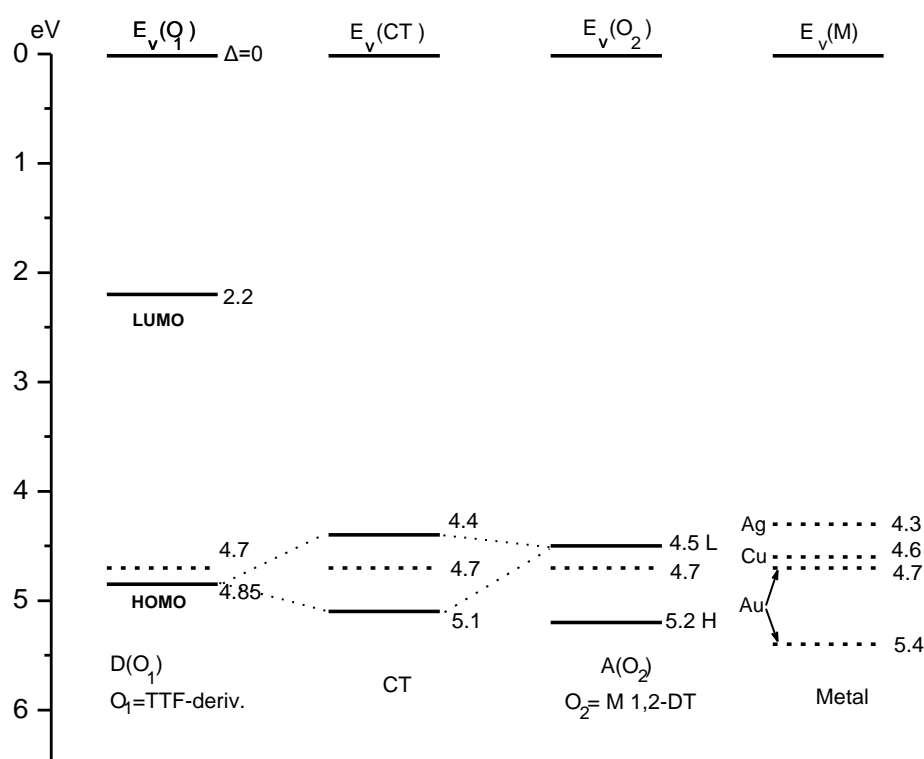
Figure 32. Energy level diagrams of metals (M), organic semiconductors (O), and metal semiconductor interfaces: work function of metals ($\Phi_{\text{Sm}} \dots \Phi_{\text{Au}}$); electron affinity (EA) of organic donor (O_1) or acceptor (O_2) and ionization energy (IE); interface potential barrier (Δ); E_v = vacuum level, Φ_e = electron injection barrier; Φ_h = hole injection barrier [7,51,66,107,127–129].



In each case of metal-semiconductor and semiconductor-insulator combinations, in order to obtain high performance FETs, alignment of LUMO and/or HOMO levels with the work function of the metal (electrode) is necessary. For example, in the case of a TTF derivative (which is a donor molecule) with a HOMO-LUMO gap of *ca.* 2.65 eV (Figure 32a) the HOMO level (4.85 eV below the vacuum level) could be in alignment with the work function of an Au electrode (which at ambient conditions is contaminated with O and C) and has a value *ca.* 4.7 eV (Figure 32b) [125]. In other words, in Au-TTF couple the hole barrier injection is small ($\Phi_h = 0.15$ eV) and holes can be injected from the HOMO level of the semiconductor to the Au electrode (p-type channel). For these kinds of compounds (donors) the electron injection barrier is large ($\Phi_e = 2.5$ eV) and injection of electrons from the Fermi level is not possible with Au electrodes. It could be possible with Sm electrodes ($\Phi_e = 0.5$ eV), but this system is not stable in air [47]. On the other hand, in TCNQ and other acceptor molecules entrapped with dicyanomethylene groups, the LUMO level occurs close to 4.3–4.4 eV and the HOMO level at 5.48–5.56 eV below the vacuum level, with a gap ≥ 1.1 eV on Au exhibit hole mobility $\mu_h = 0.014$ cm²/Vs [126]. However, in the case of M 1,2-DTs the HOMO-LUMO gap is smaller (*ca.* 0.7 eV) and the work function of Au could be aligned with both HOMO and LUMO levels (Figure 32c–e). The Φ_h and Φ_e are small and holes (p-type channel) or electrons (n-type channel) or both of them (ambipolar) could be injected. In some cases, the alignment is controlled by changing the material-semiconductor interface barrier (Δ), which leads to the change of Φ_h and Φ_e of FET [127–129].

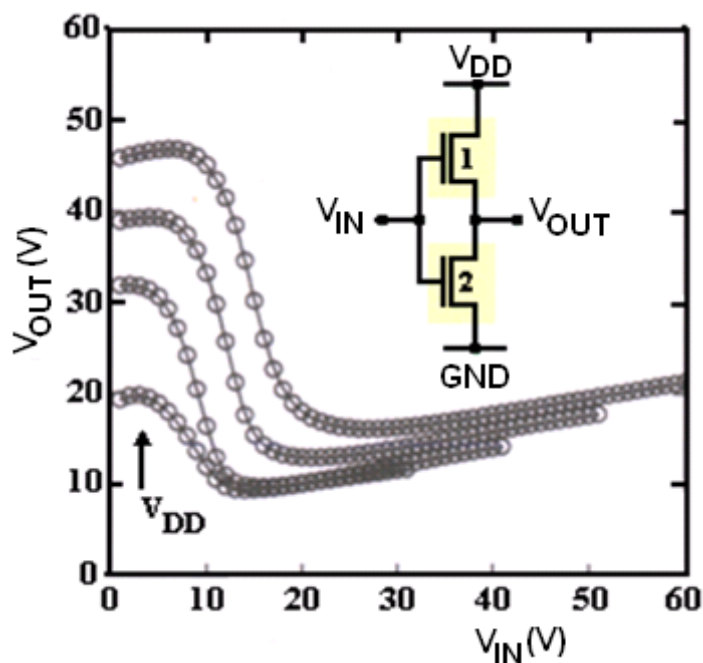
It has been demonstrated that self-assembled monolayers (SAMs), e.g., alkanethiols and perfluorinated alkanethiols have opposite dipoles and could be used to, respectively, decrease and increase the work function of metals (*i.e.*, shift the vacuum energy levels as in Figure 32c,d). This method (of SAMs) could be applied in the case of clean Au, Mo and other electrodes in which the work function is close to 5.0 eV [125]. Also, the additional edge groups in the ligands of M 1,2-DTs play more or less a role similar to that of SAMs. Moreover, during recent years, measurements under condition of FET have been performed on CT complexes of the type TTF-TCNQ [66,135,136]. However, according to our knowledge, there is no information for similar measurements on CT of the type TTF-M 1,2-DTs [15]. However, it is expected there is an alignment of the energy gap levels of these kinds of CT complexes with the work function of Au and other metals, as is illustrated in Figure 33. One can see that both Φ_e and Φ_h values could be different from those of the corresponding M 1,2-DTs. Of course, for dimerized M 1,2-DTs the diagrams are different.

Figure 33. Energy level diagram for a possible alignment of Au with the electronic levels of CT of the type TTF-M 1,2-DT [7,51,66,107,127–129].



Although, the mobility observed up to now from FETs based on M 1,2-DTs is small in comparison to that of FETs on porous silicon ($\mu_h = 1 \text{ cm}^2/\text{Vs}$), it has been demonstrated that the ambipolar semiconductors [Ni(dpdt)(dmit)] and [Ni(L10a)₂] (with $\mu_e = \mu_h \approx 10^{-3} \text{ cm}^2/\text{Vs}$) could be used for fabrication inverters, which are the main components of complementary-like circuits [37,47]. Figure 34 shows the quasi static transfer curves obtained by integrating two FETs based on [Ni(dpdt)(dmit)] (inset of Figure 33), for V_{IN} and V_{DD} being positively biased. Similar curves have been obtained for V_{IN} and V_{DD} being negatively biased.

Figure 34. Transfer curves of an ambipolar-like inverter made from two identical FETs of [Ni(dpdt)(dmit)] at ambient conditions for V_{IN} and V_{DD} being positively biased $V_{DD} = 15\text{--}60\text{ V}$ [47,77].



7. Conclusions

This paper is an overview, of the preparations and properties of neutral metal 1,2-dithiolenes (and selenium analogues). It has been shown that, using CS_2 , CSe_2 , 1,3-dithio-2 thiones, vinylene trithiocarbonate, 1,2 diketones, *etc.* as starting materials, a plethora of anionic metal 1,2-dithiolenes (and selenium analogues) could be prepared by chemical and electrochemical methods. From the anionic complexes the corresponding neutral complexes could be obtained by chemical oxidation and/or electro-oxidation. In a large number of them, the HOMO-levels are close to 4.4 eV and LUMO-levels close to 5.4 eV, forming a gap of *ca.* 1 eV. These complexes are stable (in air) semiconductors and found to be useful candidate materials for further investigation with possible applications. Their solutions, suspensions or thin deposits exhibit strong OA bands in the near-IR spectral region and have NLO properties. They can be used as saturable absorbers for telecommunication wavelength lasers (e.g., 1550 nm). Channels in FETs, made from these kinds of materials, in single crystal or thin film forms, exhibit n-type (electron) or ambipolar (electron and hole) mobilities. Some of them could be used for fabrication of inverters for complementary-like circuits. It is expected that in the near future new tailored systems, based on M-1,2 DTs with optimum properties, suitable for applications will be synthesized.

Acknowledgements

We thank Tatsuo Hasegawa and Yukihiro Takahashi for making available the single crystal electrical data prior to publication. Also, we thank the American Chemical Society, American Institute of Physics,

Elsevier, Royal Society of Chemistry and Verlag der Zeitschrift für Naturforschung for permission to reproduce diagrams in Figures 25, 28, 9 as well as 16, 10, and 12, 13, 14, 17, 22, 26, 27, respectively.

References

1. Schrauzer, G.N.; Mayweg, V.P. Reaction of diphenylacetylene with nickel sulfides. *J. Am. Chem. Soc.* **1962**, *84*, 3221.
2. Schrauzer, G.N.; Mayweg, V.P. Preparation, reactions, and structure of bisdithio- α -diketone complexes of nickel, palladium, and platinum. *J. Am. Chem. Soc.* **1965**, *87*, 1483–1489.
3. Sartain, D.; Truter, M.R. Crystal structure of bis(dithiobenzil)nickel. *J. Chem. Soc.* **1967**, doi:10.1039/j19670001264.
4. McCleverty, J.A. Metal 1,2-dithiolenes and related compounds. *Prog. Inorg. Chem.* **1968**, *10*, 49–156.
5. Underhill, A.E.; Ahmad, M.M. A new one-dimensional metal with conduction through bis(dicyanoethylenedithiolato)platinum anions. *J. Chem. Soc. Chem. Commun.* **1981**, doi:10.1039/c39810000067.
6. Papavassiliou, G.C. Some new conducting solids: Cation-deficient metal dimercaptodithiolenes and selenium analogs. *Z. Naturforsch.* **1982**, *37b*, 825–827.
7. Alvarez, S.; Vicente, R.; Hoffmann, R. Dimerization and stacking in transition-metal bisdithiolenes and tetrathiolates. *J. Am. Chem. Soc.* **1985**, *107*, 6253–6277.
8. Clemenson, P.I. The chemistry and solid-state properties of nickel, palladium and platinum bis(maleonitriledithiolate) compounds. *Coord. Chem. Rev.* **1990**, *106*, 171–203.
9. Papavassiliou, G.C.; Kakoussis, V.G.; Lagouvardos, D.J.; Mousdis, G.A. Transition-metal 1,2-diheterolenes and polyheterotetraheterafulvalenes: Precursors of conducting solids. *Mol. Cryst. Liqid Cryst.* **1990**, *181*, 171–184.
10. Muellerwesterhoff, U.T.; Vance, B.; Yoon, D.I. The synthesis of dithiolene dyes with strong near-IR absorption. *Tetrahedron* **1991**, *47*, 909–932.
11. Olk, R.M.; Olk, B.; Dietzsch, W.; Kirmse, R.; Hoyer, E. The chemistry of 1,3-dithiole-2-thione-4,5-dithiolate (dmit). *Coord. Chem. Rev.* **1992**, *117*, 99–131.
12. Papavassiliou, G.C.; Terzis, A.; Delhaes, P. Tetrachalcogenafulvalenes, metal 1,2-dichalcogenolenes and their conducting salts. *Handbook of Organic Conductive Molecules and Polymers*; Nalwa, H.S., Ed.; John Wiley & Sons: Hoboken, NJ, USA, 1997; Volume 1, pp. 152–214.
13. Kotov, A.I.; Buravov, L.I.; Yagubskii, E.B.; Khasanov, S.S.; Zorina, L.V.; Shibaeva, R.P.; Canadell, E. Comparative study of BEDT TTF and Ni(ddd)₂ electroconducting salts with the HXO₄ (X = Se, S) anions. *Synth. Met.* **2001**, *124*, 357–362.
14. Watanabe, E.; Fujiwara, M.; Yamaura, J.; Kato, R. Synthesis and properties of novel donor-type metal-dithiolene complexes based on 5,6-dihydro-1,4-dioxine-2,3-dithiol (edo). *J. Mater. Chem.* **2001**, *11*, 2131–2141.
15. Robertson, N.; Cronin, L. Metal bis-1,2-dithiolene complexes in conducting or magnetic crystalline assemblies. *Coord. Chem. Rev.* **2002**, *227*, 93–127.

16. Papavassiliou, G.C. Tetrachalcogenafulvalenes with four additional heteroatoms. In *TTF Chemistry: Fundamentals and Applications of Tetrathiafulvalene*; Yamada, J.-I., Sugimoto, T., Eds.; Springer: Berlin, Germany, 2004; pp. 35–58.
17. Beswick, C.L.; Schulman, J.M.; Stiefel, E.I. Structures and structural trends in homoleptic dithiolene complexes. In *Dithiolene Chemistry: Synthesis, Properties, and Applications*; Stiefel, E.I., Ed.; John Wiley & Sons: Hoboken, NJ, USA, 2004; Volume 52, pp. 55–110.
18. Kirk, M.L.; McNaughton, R.L.; Helton, M.E. The electronic structure and spectroscopy of metallo-dithiolene complexes. *Prog. Inorg. Chem.* **2004**, *52*, 111–212.
19. Wang, K. Electrochemical and chemical reactivity of dithiolene complexes. *Prog. Inorg. Chem.* **2004**, *52*, 267–314.
20. Faulmann, C.; Cassoux, P. Solid-state properties (electronic, magnetic, optical) of dithiolene complex-based compounds. *Prog. Inorg. Chem.* **2004**, *52*, 399–489.
21. Kato, R. Conducting metal dithiolene complexes: Structural and electronic properties. *Chem. Rev.* **2004**, *104*, 5319–5346.
22. Fujiwara, E.; Kobayashi, A.; Fujiwara, H.; Kobayashi, H. Syntheses, structures, and physical properties of nickel bis(dithiolene) complexes containing tetrathiafulvalene (TTF) units. *Inorg. Chem.* **2004**, *43*, 1122–1129.
23. Kobayashi, A.; Fujiwara, E.; Kobayashi, H. Single-component molecular metals with extended-TTF dithiolate ligands. *Chem. Rev.* **2004**, *104*, 5243–5264.
24. Aragoni, M.C.; Arca, M.; Caironi, M.; Denotti, C.; Devillanova, F.A.; Grigiotti, E.; Isaia, F.; Laschi, F.; Lippolis, V.; Natali, D.; *et al.* Monoreduced [M(R,R' timdt)(2)]-dithiolenes (M = Ni, Pd, Pt; R,R' timdt = disubstituted imidazolidine-2,4,5-trithione): Solid state photoconducting properties in the third optical fiber window. *Chem. Commun.* **2004**, doi:10.1039/B406406B.
25. Pearson, C.; Moore, A.J.; Gibson, J.E.; Bryce, M.R.; Petty, M.C. A Field-effect transistor based on Langmuir-Blodgett-films of an Ni(dmit)₂ charge-transfer complex. *Thin Solid Films* **1994**, *244*, 932–935.
26. Tenn, N.; Bellec, N.; Jeannin, O.; Piekara-Sady, L.; Auban-Senzier, P.; Íniguez, J.; Canadell, E.; Lorcy, D. A single-component molecular metal based on a thiazole dithiolate gold complex. *J. Am. Chem. Soc.* **2009**, *131*, 16961–16967.
27. Papavassiliou, G.C.; Anyfantis, G.C. Alternative method for the preparation of Ni(dddt)(edt) (dddt = 5,6-dihydro-1,4-dithiin-2,3-dithiolate, edt = *cis*-1,2-ethylenedithiolate) and similar complexes. *Z. Naturforsch.* **2005**, *60b*, 811–813.
28. Ji, Y.; Zuo, J.L.; Chen, L.X.; Tian, Y.Q.; Song, Y.L.; Li, Y.Z.; You, X.Z. Synthesis, characterization and optical limiting effect of nickel complexes of multi-sulfur 1,2-dithiolene. *J. Phys. Chem. Solids* **2005**, *66*, 207–212.
29. Schiodt, N.C.; Bjornholm, T.; Bechgaard, K.; Neumeier, J.J.; Allgeier, C.; Jacobsen, C.S.; Thorup, N. Structural, electrical, magnetic, and optical properties of bis-benzene-1,2-dithiolato-Au(IV) crystals. *Phys. Rev.* **1996**, *53*, 1773–1778.
30. Papavassiliou, G.C. Design and synthesis of polyheterotetraheterafulvalenes metal 1,2 diheterolenes, and their low-dimensional conducting and superconducting salts. In *Lower-Dimensional Systems and Molecular Electronics (NATO Science Series B)*; Metzger, R.M., Day, P., Papavassiliou, G.C., Eds.; Springer: Berlin, Germany, 1990; pp. 143–162.

31. Aragoni, M.C.; Arca, M.; Devillanova, F.A.; Isaia, F.; Lippolis, V.; Mancini, A.; Pala, L.; Slawin, A.M.Z.; Woollins, J.D. [M(R-dmet)₂] bis(1,2-dithiolenes): A promising new class intermediate between [M(dmit)₂] and [M(R,R'-timdt)₂] (M = Ni, Pd, Pt). *Inorg. Chem.* **2005**, *44*, 9610–9612.
32. Matsubayashi, G.; Maikawa, T.; Nakano, M. Preparation, spectroscopy and oxidation of [Re(C₃S₅)₃]- and [ReO(C₃S₅)₂]-complexes and crystal-structure of [PPh₄][ReO(C₃S₅)₂]. *J. Chem. Soc. Dalton Trans.* **1993**, doi:10.1039/DT9930002995.
33. Caironi, M.; Natali, D.; Sampietro, M.; Ward, M.; Meacham, A.; Devillanova, F.A.; Arca, M.; Denotti, C.; Pala, L. Near infrared detection by means of coordination complexes. *Synth. Met.* **2005**, *153*, 273–276.
34. Ray, K.; Weyhermuller, T.; Neese, F.; Wieghardt, K. Electronic structure of square planar bis(benzene-1,2-dithiolato)metal complexes [M(L)^{2z}] (z = 2-, 1-, 0; M = Ni, Pd, Pt, Cu, Au): An experimental, density functional, and correlated *ab initio* study. *Inorg. Chem.* **2005**, *44*, 5345–5360.
35. Tanaka, H.; Okano, Y.; Kobayashi, H.; Suzuki, W.; Kobayashi, A. A three-dimensional synthetic metallic crystal composed of single-component molecules. *Science* **2001**, *291*, 285–287.
36. Anyfantis, G.C.; Papavassiliou, G.C.; Terzis, A.; Raptopoulou, C.P.; Weng, Y.F.; Yoshino, H.; Murata, K. Preparation and characterization of some nickel 1,2-dithiolene complexes as single-component semiconductors. *Z. Naturforsch.* **2006**, *61b*, 1007–1011.
37. Anthopoulos, T.D.; Setayesh, S.; Smits, E.; Colle, M.; Cantatore, E.; de Boer, B.; Blom, P.W.M.; de Leeuw, D.M. Air-stable complementary-like circuits based on organic ambipolar transistors. *Adv. Mater.* **2006**, *18*, 1900–1904.
38. Smits, E.C.P.; Anthopoulos, T.D.; Setayesh, S.; van Veenendaal, E.; Coehoorn, R.; Blom, P.W.M.; de Boer, B.; de Leeuw, D.M. Ambipolar charge transport in organic field-effect transistors. *Phys. Rev.* **2006**, *73*, 205316–205321.
39. Taguchi, T.; Wada, H.; Kambayashi, T.; Noda, B.; Goto, M.; Mori, T.; Ishikawa, K.; Takezoe, H. Comparison of p-type and n-type organic field-effect transistors using nickel coordination compounds. *Chem. Phys. Lett.* **2006**, *421*, 395–398.
40. Nakano, M.; Kuroda, A.; Matsubayashi, G. Extended bisdithiolene metal complexes: Preparation and electrical conductivities of [M(C₈H₄S₈)₂] anion complexes. *Inorg. Chim. Acta* **1997**, *254*, 189–193.
41. Marshall, K.L.; Painter, G.; Lotito, K.; Noto, A.G.; Chang, P. Transition metal dithiolene near-IR dyes and their applications in liquid crystal devices. *Mol. Cryst. Liquid Cryst.* **2006**, *454*, 47–79.
42. Barriere, F.; Geiger, W.E. Use of weakly coordinating anions to develop an integrated approach to the tuning of ΔE_{1/2} values by medium effects. *J. Am. Chem. Soc.* **2006**, *128*, 3980–3989.
43. Zhou, B.; Yajima, H.; Idobata, Y.; Kobayashi, A.; Kobayashi, T.; Nishibori, E.; Sawa, H.; Kobayashi, H. Single-component layered molecular conductor, [Au(ptdt)₂]. *Chem. Lett.* **2012**, *41*, 154–156.
44. Im, J.U.; Yu, C.Y.; Yoo, J.Y.; Son, S.M.; Lee, G.D.; Park, S.S. A study for microwave enhanced synthesis of NIR absorbing materials. *Mater. Sci. Forum* **2006**, *510–511*, 702–705.
45. Kobayashi, A.; Okano, Y.; Kobayashi, H. Molecular design and physical properties of single-component molecular metals. *J. Phys. Soc. Jpn.* **2006**, *75*, doi:10.1143/JPSJ.75.051002.

46. Kobayashi, A.; Kobayashi, H. Single-component molecular conductors. *Mol. Cryst. Liquid Cryst.* **2006**, *455*, 47–56.
47. Anthopoulos, T.D.; Anyfantis, G.C.; Papavassiliou, G.C.; de Leeuw, D.M. Air-stable ambipolar organic transistors. *Appl. Phys. Lett.* **2007**, *90*, doi:10.1063/1.2715028.
48. Anyfantis, G.C.; Papavassiliou, G.C.; Aloukos, P.; Couris, S.; Weng, Y.F.; Yoshino, H.; Murata, K. Unsymmetrical single-component nickel 1,2-dithiolene complexes with extended tetrachalcogenafulvalenedithiolato ligands. *Z. Naturforsch.* **2007**, *62b*, 200–204.
49. Papavassiliou, G.C.; Anyfantis, G.C.; Koutselas, I.B. Some air-stable unsymmetrical nickel 1,2-dithiolenes with extended tetrathiafulvalenedithiolato ligands. *Z. Naturforsch.* **2007**, *62b*, 1481–1486.
50. Papavassiliou, G.C.; Anyfantis, G.C.; Steele, B.R.; Terzis, A.; Raptopoulou, C.P.; Tatakis, G.; Chaidogiannos, G.; Glezos, N.; Weng, Y.F.; Yoshino, H.; Murata, K. Some new nickel 1,2-dichalcogenolene complexes as single-component semiconductors. *Z. Naturforsch.* **2007**, *62b*, 679–684.
51. Saito, G.; Yoshida, Y. Development of conductive organic molecular assemblies: Organic metals, superconductors, and exotic functional materials. *Bull. Chem. Soc. Jpn.* **2007**, *80*, 1–137.
52. Papavassiliou, G.C.; Mousdis, G.A.; Anyfandis, G.C. An improved synthesis of nickel-bis [5,6-dihydro-1,4-dioxine-2,3-dithiolate], Ni(edo)₂. *Z. Naturforsch.* **2002**, *57b*, 707–708.
53. Nunes, J.P.M.; Figueira, M.J.; Belo, D.; Santos, I.C.; Ribeiro, B.; Lopes, E.B.; Henriques, R.T.; Vidal-Gancedo, J.; Veciana, J.; Rovira, C.; *et al.* Transition metal bisdithiolene complexes based on extended ligands with fused tetrathiafulvalene and thiophene moieties: New single-component molecular metals. *Chem. Eur. J.* **2007**, *13*, 9841–9849.
54. Papavassiliou, G.C.; Cotsilios, A.M.; Jacobsen, C.S. Spectroscopic investigation of metal dimercaptodithiolenes and selenium analogs. *J. Mol. Struct.* **1984**, *115*, 41–44.
55. Eid, S.; Fourmigue, M.; Roisnel, T.; Lorcey, D. Influence of the thiazole backbone on the structural, redox, and optical properties of dithiolene and diselenolene complexes. *Inorg. Chem.* **2007**, *46*, 10647–10654.
56. Wada, H.; Taguchi, T.; Noda, B.; Kambayashi, T.; Mori, T.; Ishikawa, K.; Takezoe, H. Air stability of n-channel organic transistors based on nickel coordination compounds. *Org. Electron.* **2007**, *8*, 759–766.
57. Cho, J.Y.; Domercq, B.; Jones, S.C.; Yu, J.; Zhang, X.; An, Z.; Bishop, M.; Barlow, S.; Marder, S.R.; Kippelen, B. High electron mobility in nickel bis(dithiolene) complexes. *J. Mater. Chem.* **2007**, *17*, 2642–2647.
58. Cho, J.Y.; Barlow, S.; Marder, S.R.; Fu, J.; Padilha, L.A.; van Stryland, E.W.; Hagan, D.J.; Bishop, M. Strong two-photon absorption at telecommunications wavelengths in nickel bis(dithiolene) complexes. *Opt. Lett.* **2007**, *32*, 671–673.
59. Agostinelli, T.; Caironi, M.; Natali, D.; Sampietro, M.; Arca, M.; Devillanova, F.A.; Ferrero, V. Trapping effects on the frequency response of dithiolene-based planar photodetectors. *Synth. Met.* **2007**, *157*, 984–987.

60. Kokatam, S.; Ray, K.; Pap, J.; Bill, E.; Geiger, W.E.; Lesuer, R.J.; Rieger, P.H.; Weyhermuller, T.; Neese, F.; Wieghardt, K. Molecular and electronic structure of square-planar gold complexes containing two 1,2-di(4-*tert*-butylphenyl)ethylene-1,2-dithiolato ligands: $[\text{Au}(\text{L}^{-2})_2](1+/0/1-/2-)$. A combined experimental and computational study. *Inorg. Chem.* **2007**, *46*, 1100–1111.
61. Rabaca, S.; Duarte, M.C.; Santos, I.C.; Fourmigue, M.; Almeida, M. A new approach to divalent thio-azo ligands; $\text{Ni}(\text{dpsdt})_2$. *Inorg. Chim. Acta* **2007**, *360*, 3797–3801.
62. Aragoni, M.C.; Arca, M.; Devillanova, F.A.; Isaia, F.; Lippolis, V.; Mancini, A.; Pala, L.; Verani, G.; Agostinelli, T.; Caironi, M.; *et al.* First example of a near-IR photodetector based on neutral $[\text{M}(\text{r-dmet})_2]$ bis(1,2-dithiolene) metal complexes. *Inorg. Chem. Commun.* **2007**, *10*, 191–194.
63. Papavassiliou, G.C.; Anyfantis, G.C.; Terzis, A.; Psycharis, V.; Kyritsis, P.; Paraskevopoulou, P. Some unsymmetrical metal 1,2-dithiolenes based on palladium, platinum and gold. *Z. Naturforsch.* **2008**, *63b*, 1377–1382.
64. Anyfantis, G.C.; Papavassiliou, G.C.; Assimomytis, N.; Terzis, A.; Psycharis, V.; Raptopoulou, C.P.; Kyritsis, P.; Thoma, V.; Koutselas, I.B. Some unsymmetrical nickel 1,2-dithiolene complexes as candidate materials for optics and electronics. *Solid State Sci.* **2008**, *10*, 1729–1733.
65. Stallinga, P.; Benvenho, A.R.V.; Smits, E.C.P.; Mathijssen, S.G.J.; Colle, M.; Gomes, H.L.; de Leeuw, D.M. Determining carrier mobility with a metal-insulator-semiconductor structure. *Org. Electron.* **2008**, *9*, 735–739.
66. Mori, T. Molecular materials for organic field-effect transistors. *J. Phys Condens. Matter* **2008**, *20*, doi:10.1088/0953-8984/20/18/184010.
67. Romaniello, P.; Dandria, M.C.; Lelj, F. Nonlinear optical properties of $\text{Ni}(\text{Me}_6\text{pzS}_2)\text{MX}$ ($\text{M} = \text{Ni, Pd, Pt}$; $\text{X} = \text{Me}_2\text{timdt, mnt}$). *J. Phys. Chem.* **2010**, *114*, 5838–5845.
68. Bruno, G.; Almeida, M.; Artizzu, F.; Dias, J.C.; Mercuri, M.L.; Pilia, L.; Rovira, C.; Ribas, X.; Serpe, A.; Deplano, P. Innocence and noninnocence of the ligands in bis(pyrazine-2,3-dithiolate and -diselonate) d^8 -metal complexes. A theoretical and experimental study for the Cu(III), Au(III) and Ni(II) cases. *Dalton Trans.* **2010**, *39*, 4566–4574.
69. Cassoux, P.; Valade, L.; Kobayashi, H.; Kobayashi, A.; Clark, R.A.; Underhill, A.E. Molecular-metals and superconductors derived from metal-complexes of 1,3-dithiol-2-thione-4,5-dithiolate (dmit). *Coord. Chem. Rev.* **1991**, *110*, 115–160.
70. Anjos, T.; Roberts-Bleming, S.J.; Charlton, A.; Robertson, N.; Mount, A.R.; Coles, S.J.; Hursthouse, M.B.; Kalaji, M.; Murphy, P.J. Nickel dithiolenes containing pendant thiophene units: Precursors to dithiolene-polythiophene hybrid materials. *J. Mater. Chem.* **2008**, *18*, 475–483.
71. Kubo, K.; Nakao, A.; Ishii, Y.; Yamamoto, T.; Tamura, M.; Kato, R.; Yakushi, K.; Matsubayashi, G.E. Electrical properties and electronic states of molecular conductors based on unsymmetrical organometallic-dithiolene gold(III) complexes. *Inorg. Chem.* **2008**, *47*, 5495–5502.
72. Cho, J.Y.; Fu, J.; Padilha, L.A.; Barlow, S.; van Stryland, E.W.; Hagan, D.J.; Bishop, M.; Marder, S.R. Synthesis of a nickel bis(dithiolene) complex with strong near-infrared two-photon absorption. *Mol. Cryst. Liquid Cryst.* **2008**, *485*, 915–927.
73. Madhu, V.; Das, S.K. New series of asymmetrically substituted bis(1,2-dithiolato)-nickel(III) complexes exhibiting near IR absorption and structural diversity. *Inorg. Chem.* **2008**, *47*, 5055–5070.

74. Sournia-Saquet, A.; Garreau-De Bonneval, B.; Chane-Ching, K.I.; Valade, L. Electrochemical properties and electronic structures of two neutral nickel bis(1,2-dithiolene) complexes. *J. Electroanal. Chem.* **2008**, *624*, 84–90.
75. Skabara, P.J.; Pozo-Gonzalo, C.; Miazza, N.L.; Laguna, M.; Cerrada, E.; Luquin, A.; Gonzalez, B.; Coles, S.J.; Hursthouse, M.B.; Harrington, R.W.; *et al.* Novel dithiolene complexes incorporating conjugated electroactive ligands. *Dalton Trans.* **2008**, doi:10.1039/B801187G.
76. Song, I.H.; Rhee, C.H.; Park, S.H.; Lee, S.L.; Grudinin, D.; Song, K.H.; Choe, J. Continuous production of a near infrared absorbing chromophore. *Org. Proc. Res. Dev.* **2008**, *12*, 1012–1015.
77. Anyfantis, G.C. Unsymmetrical Metal 1,2-Dithiolenes: Design, Synthesis, Properties and Possible Applications. Ph.D. Thesis, University of Patras, Patras, Greece, 2008.
78. Nishikawa, H.; Yasuoka, W.; Sakairi, K.; Oshio, H. Synthesis and physical properties of a new single-component molecular conductor [Au(dhdt)₂]. *Polyhedron* **2009**, *28*, 1634–1637.
79. Papavassiliou, G.C.; Anyfantis, G.C.; Raptopoulou, C.P.; Psycharis, V.; Ioannidis, N.; Petrouleas, V.; Paraskevopoulou, P. Bis[1,2-diphenyl-1,2-ethylenedithiolato(2⁻)-kS₁,kS₂] gold: Preparation, structure and properties. *Polyhedron* **2009**, *28*, 3368–3372.
80. Deplano, P.; Marchio, L.; Artizzu, F.; Mercuri, M.L.; Pilia, L.; Pintus, G.; Serpe, A.; Yagubskii, E.B. Square-planar mixed ligand nickel dithiolenes as second-order non-linear chromophores: Synthesis and characterisation of [Ni(Me₂pipdt)(ddd)]. *Monatsh. Chem.* **2009**, *140*, 775–781.
81. Arumugam, K.; Shaw, M.C.; Chandrasekaran, P.; Villagran, D.; Gray, T.G.; Mague, J.T.; Donahue, J.P. Synthesis, structures, and properties of 1,2,4,5-benzenetetrathiolate linked group 10 metal complexes. *Inorg. Chem.* **2009**, *48*, 10591–10607.
82. Charrier, D.S.H.; de Vries, T.; Mathijssen, S.G.J.; Geluk, E.J.; Smits, E.C.P.; Kemerink, M.; Janssen, R.A.J. Bimolecular recombination in ambipolar organic field effect transistors. *Org. Electron.* **2009**, *10*, 994–997.
83. Dalgleish, S.; Robertson, N. A stable near IR switchable electrochromic polymer based on an indole-substituted nickel dithiolene. *Chem. Commun.* **2009**, doi:10.1039/B913174D.
84. Perochon, R.; Poriel, C.; Jeannin, O.; Piekara-Sady, L.; Fourmigue, M. Chiral, neutral, and paramagnetic gold dithiolene complexes derived from camphorquinone. *Eur. J. Inorg. Chem.* **2009**, *2009*, 5413–5421.
85. Serrano-Andres, L.; Avramopoulos, A.; Li, J.B.; Labeguerie, P.; Begue, D.; Kello, V.; Papadopoulos, M.G. Linear and nonlinear optical properties of a series of Ni-dithiolene derivatives. *J. Chem. Phys.* **2009**, *131*, doi:10.1063/1.3238234.
86. Tamura, M.; Kato, R. Variety of valence bond states formed of frustrated spins on triangular lattices based on a two-level system Pd(dmit)₂. *Sci. Technol. Adv. Mater.* **2009**, *10*, doi:10.1088/1468-6996/10/2/024304.
87. Tenn, N.; Bellec, N.; Jeannin, O.; Piekara-Sady, L.; Auban-Senzier, P.; Iniguez, J.; Canadell, E.; Lorcy, D. A single-component molecular metal based on a thiazole dithiolate gold complex. *J. Am. Chem. Soc.* **2009**, *131*, 16961–16967.
88. Pilia, L.; Artizzu, F.; Faulmann, C.; Mercuri, M.L.; Serpe, A.; Deplano, P. Square-planar d⁸ metal push-pull dithiolene complexes: Synthesis and characterization of [Pd(Me₂pipdt)(dmit)]. *Inorg. Chem. Commun.* **2009**, *12*, 490–493.

89. Perochon, R.; Piekara-Sady, L.; Jurga, W.; Clerac, R.; Fourmigue, M. Amphiphilic paramagnetic neutral gold dithiolene complexes. *Dalton Trans.* **2009**, doi:10.1039/B820819K.
90. Zhou, B.; Kobayashi, A.; Okano, Y.; Nakashima, T.; Aoyagi, S.; Nishibori, E.; Sakata, M.; Tokumoto, M.; Kobayashi, H. Single-component molecular conductor [Pt(tmdt)(2)] (tmdt = trime thylenetetrafulvalenedithiolate)—An advanced molecular metal exhibiting high metallicity. *Adv. Mater.* **2009**, *21*, 3596–3600.
91. Bruno, G.; Almeida, M.; Simao, D.; Mercuri, M.L.; Pilia, L.; Serpe, A.; Deplano, P. Peculiar electronic and vibrational properties of metal-dithiolenes (Ni, Au) based on 1,2,5-thiadiazole-3, 4-dithiolato. *Dalton Trans.* **2009**, doi:10.1039/B812214H.
92. Soras, G.; Psaroudakis, N.; Manos, M.J.; Tasiopoulos, A.J.; Liakos, D.G.; Mousdis, G.A. New type dithiolene complex based on 4,5-(1,4-dioxane-2,3-diylidithio)-1,3-dithiol ligand: Synthesis, experimental and theoretical investigation. *Polyhedron* **2009**, *28*, 3340–3348.
93. Dalgleish, S.; Yoshikawa, H.; Matsushita, M.M.; Awaga, K.; Robertson, N. Electrodeposition as a superior route to a thin film molecular semiconductor. *Chem. Sci.* **2011**, *2*, 316–320.
94. Anyfantis, G.C.; Papavassiliou, G.C.; Terzis, A.; Raptopoulou, C.P.; Psycharis, V.; Paraskevopoulou, P. Preparation and characterization of Ni(dpdt)(pddt) and Ni(dpdt)(pddt) CS₂, where dpdt is diphenylethylenedithiolate and pddt is 6,7-dihydro-5H-1,4-dithiepin-2,3-dithiolate. *Polyhedron* **2010**, *29*, 969–974.
95. Deplano, P.; Pilia, L.; Espa, D.; Mercuri, M.L.; Serpe, A. Square-planar d⁸ metal mixed-ligand dithiolene complexes as second order nonlinear optical chromophores: Structure/property relationship. *Coord. Chem. Rev.* **2009**, *254*, 1434–1447.
96. Ambrosio, L.; Aragoni, M.C.; Arca, M.; Devillanova, F.A.; Hursthouse, M.B.; Huth, S.L.; Isaia, F.; Lippolis, V.; Mancini, A.; Pintus, A. Synthesis and characterization of novel gold(III) complexes of asymmetrically aryl-substituted 1,2-dithiolene ligands featuring potential-controlled spectroscopic properties. *Chem. Asian J.* **2010**, *5*, 1395–1406.
97. Rabaca, S.; Almeida, M. Dithiolene complexes containing n coordinating groups and corresponding tetrathiafulvalene donors. *Coord. Chem. Rev.* **2010**, *254*, 1493–1508.
98. Basu, P.; Nigam, A.; Mogesa, B.; Denti, S.; Nemykin, V.N. Synthesis, characterization, spectroscopy, electronic and redox properties of a new nickel dithiolene system. *Inorg. Chim. Acta* **2010**, *363*, 2857–2864.
99. Aloukos, P.; Chatzikyriakos, G.; Papagiannouli, I.; Liaros, N.; Couris, S. Transient nonlinear optical response of some symmetrical nickel dithiolene complexes. *Chem. Phys. Lett.* **2010**, *495*, 245–250 and references therein.
100. Soras, G.; Psaroudakis, N.; Mousdis, G.A.; Manos, M.J.; Tasiopoulos, A.J.; Aloukos, P.; Couris, S.; Labeguerie, P.; Lipinski, J.; Avramopoulos, A.; *et al.* Synthesis and non-linear optical properties of some novel nickel derivatives. *Chem. Phys.* **2010**, *372*, 33–45.
101. Bui, T.T.; Garreau-De Bonneval, B.; Ching, K. Synthesis and preliminary physical properties of new neutral tetraalkoxy-substituted nickel bis(1,2-dithiolene) complexes. *New J. Chem.* **2010**, *34*, 337–347.
102. Garreau-De Bonneval, B.; Ching, K.; Alary, F.; Bui, T.T.; Valade, L. Neutral d⁸ metal bis-dithiolene complexes: Synthesis, electronic properties and applications. *Coord. Chem. Rev.* **2010**, *254*, 1457–1467.

103. Chatzikyriakos, G.; Papagiannouli, I.; Couris, S.; Anyfantis, G.C.; Papavassiliou, G.C. Nonlinear optical response of a symmetrical au dithiolene complex under ps and ns laser excitation in the infrared and in the visible. *Chem. Phys. Lett.* **2011**, *513*, 229–235.
104. Aragoni, M.C.; Arca, M.; Devillanova, F.A.; Isaia, F.; Lippolis, V.; Pintus, A. Gold(III) complexes of asymmetrically aryl-substituted 1,2-dithiolene ligands featuring potential-controlled spectroscopic properties: An insight into the electronic properties of bis(pyren-1-yl-ethylene-1,2-dithiolato)gold(III). *Chem. Asian J.* **2011**, *6*, 198–208.
105. Takahashi, Y.; Hasegawa, T.; Papavassiliou, G.C.; Anyfantis, G.C. Single crystal FETs based on metal 1,2-dithiolenes. National Hellenic Research Foundation, Greece. Unpublished Work, 2012.
106. Pilia, L.; Espa, D.; Barsella, A.; Fort, A.; Makedonas, C.; Marchio, L.; Mercuri, M.L.; Serpe, A.; Mitsopoulou, C.A.; Deplano, P. Combined experimental and theoretical study on redox-active d^8 metal dithione-dithiolato complexes showing molecular second-order nonlinear optical activity. *Inorg. Chem.* **2011**, *50*, 10015–10027.
107. Mori, T. Organic charge-transfer salts and the component molecules in organic transistors. *Chem. Lett.* **2011**, *40*, 428–434.
108. Starodub, V.A.; Starodub, T.N. Isotrithionedithiolate transition metal complexes. *Russ. Chem. Rev.* **2011**, *80*, 829–853.
109. Dalgleish, S.; Awaga, K.; Robertson, N. Formation of stable neutral copper bis-dithiolene thin films by potentiostatic electrodeposition. *Chem. Commun.* **2011**, *47*, 7089–7091.
110. Miao, Q.; Gao, J.; Wang, Z.; Yu, H.; Luo, Y.; Ma, T. Syntheses and characterization of several nickel bis(dithiolene) complexes with strong and broad near-IR absorption. *Inorg. Chim. Acta* **2011**, *376*, 619–627.
111. Eisenberg, R.; Gray, B.G. Noninnocence in metal complexes: A dithiolene dawn. *Inorg. Chem.* **2011**, *50*, 9741–9751.
112. Espa, D.; Pilia, L.; Marchio, L.; Mercuri, M.L.; Serpe, A.; Barsella, A.; Fort, A.; Dalgleish, S.J.; Robertson, N.; Deplano, P. Redox-switchable chromophores based on metal (Ni, Pd, Pt) mixed-ligand dithiolene complexes showing molecular second-order nonlinear-optical activity. *Inorg. Chem.* **2011**, *50*, 2058–2060.
113. Dalgleish, S.; Labram, J.G.; Li, Z.; Wang, J.P.; Mcneill, C.R.; Anthopoulos, T.D.; Greenham, N.C.; Robertson, N. Indole-substituted nickel dithiolene complexes in electronic and optoelectronic devices. *J. Mater. Chem.* **2011**, *21*, 15422–15430.
114. Hu, L.; Qin, J.; Zhou, N.; Meng, Y.-F.; Xu, Y.; Zuo, J.-L.; You, X.-Z. Synthesis, characterization, and optical properties of new metal complexes with the multi-sulfur 1,2-dithiolene ligand. *Dye. Pigment.* **2012**, *92*, 1223–1230.
115. Stout, G.H.; Jensen, L.H. *X-Ray Structure Determination*, 2nd ed.; John Wiley & Sons: Hoboken, NJ, USA, 1989; Chapter 4, p. 74.
116. Kalb, W.L.; Mattenberger, K.; Batlogg, B. Oxygen-related traps in pentacene thin films: Energetic position and implications for transistor performance. *Phys. Rev.* **2008**, *78*, doi:10.1103/PhysRevB.78.035334.
117. Williams, J.M.; Ferraro, J.R.; Thorn, R.J.; Carlson, K.D.; Geiser, U.; Wang, H.H.; Kini, A.M.; Whangbo, M.H. *Organic Superconductors (including Fullerenes) Synthesis, Structure, Properties and Theory*; Prentice Hall: Englewood Cliffs, NJ, USA, 1992.

118. Papavassiliou, G.C. Optical-properties of small inorganic and organic metal particles. *Prog. Solid State Chem.* **1979**, *12*, 185–271.
119. Papavassiliou, G.C. Three- and low-dimensional inorganic semiconductors. *Prog. Solid State Chem.* **1997**, *25*, 125–270.
120. Bawendi, M.G.; Steigerwald, M.L.; Brus, L.E. The quantum-mechanics of larger semiconductor clusters (quantum dots). *Annu. Rev. Phys. Chem.* **1990**, *41*, 477–496.
121. Rozhin, A.G.; Scardaci, V.; Wang, F.; Hennrich, F.; White, I.H.; Milne, W.I.; Ferrari, A.C. Generation of ultra-fast laser pulses using nanotube mode-lockers. *Phys. Status Solidi B* **2006**, *243*, 3551–3555.
122. Ward, M.D. Electrochemical Aspects of Low-Dimensional Molecular Solids. In *Electroanalytical Chemistry*; Bard, A.J., Ed.; Dekker: New York, NY, USA, 1988; Volume 16, pp. 182–299.
123. Fraboni, B.; Femoni, C.; Mencarelli, I.; Setti, L.; Di Pietro, R.; Cavallini, A.; Fraleoni-Morgera, A. Solution-grown, macroscopic organic single crystals exhibiting three-dimensional anisotropic charge-transport properties. *Adv. Mater.* **2009**, *21*, 1835–1839.
124. Podzorov, V.; Pudalov, V.M.; Gershenson, M.E. Field-effect transistors on rubrene single crystals with parylene gate insulator. *Appl. Phys. Lett.* **2003**, *82*, 1739–1741.
125. Wan, A.; Hwang, J.; Amy, F.; Kahn, A. Impact of electrode contamination on the α -NPD/Au hole injection barrier. *Org. Electron.* **2005**, *6*, 47–54.
126. Qiao, Y.; Zhang, J.; Xu, W.; Zhu, D. Incorporation of pyrrole to oligothiophene-based quinoids end capped with dicyanomethylene: A new class of solution processable n-channel organic semiconductors for air-stable organic field-effect transistors. *J. Mater. Chem.* **2012**, in press.
127. Kahn, A.; Koch, N.; Gao, W.Y. Electronic structure and electrical properties of interfaces between metals and pi-conjugated molecular films. *J. Polym. Sci. B Polym Phys.* **2003**, *41*, 2529–2548.
128. Braun, S.; Salaneck, W.R.; Fahlman, M. Energy-level alignment at organic/metal and organic/organic interfaces. *Adv. Mater.* **2009**, *21*, 1450–1472.
129. Rhee, S.W.; Yun, D.J. Metal-semiconductor contact in organic thin film transistors. *J. Mater. Chem.* **2008**, *18*, 5437–5444.
130. Papavassiliou, G.C.; Kakoussis, V.C.; Lagouvardos, D.J. Preparation of some bis(alkylthio)-bis(alkylseleno)tetrathiafulvalenes. *Z. Naturforsch.* **1991**, *46b*, 1269–1271.
131. Papavassiliou, G.C.; Lagouvardos, D.J.; Kakoussis, V.C. 5,6-Ethylenediseleno-1,3-dithiolo[4,5-*b*] [1,4]dithiin-2-thione as starting material for the preparation of new tetrathiafulvalenes. *Z. Naturforsch.* **1991**, *46b*, 1730–1732.
132. Papavassiliou, G.C.; Misaki, Y.; Takahashi, K.; Yamada, J.; Mousdis, G.A.; Sharahata, T.; Ise, T. New pi-donor molecules with a pyrazino group and their conducting salts. *Z. Naturforsch.* **2001**, *56b*, 297–300.
133. Yamada, J.-I.; Sugimoto, T. *TTF Chemistry: Fundamentals and Applications of Tetrathiafulvalene*; Springer: Berlin, Germany, 2004.
134. Akhrem, A.A.; Govorova, A.A.; Gulyakevich, O.V.; Lyakhov, A.S.; Mikhal'chuk, A.L.; Skorniyakov, I.V.; Tolstorozhev, G.B. Intermolecular interactions of immunoactive 8-azasteroid. *Opt. Spectrosc.* **2005**, *99*, 74–80.

135. Takahashi, Y.; Hasegawa, J.; Abe, Y.; Tokura, Y.; Nishimura, K.; Saito, G. Tuning of electron injections for n-type organic transistor based on charge-transfer compounds. *Appl. Phys. Lett.* **2005**, *86*, doi:10.1063/1.1863434.
136. Takahashi, Y.; Hasegawa, T.; Abe, Y.; Tokura, Y.; Saito, G. Organic metal electrodes for controlled p- and n-type carrier injections in organic field-effect transistors. *Appl. Phys. Lett.* **2006**, *88*, doi:10.1063/1.2173226.
137. Takahashi, Y.; Hasegawa, T.; Horiuchi, S.; Kumai, R.; Tokura, Y.; Saito, G. High mobility organic field-effect transistor based on hexamethylenetetrafulvalene with organic metal electrodes. *Chem. Mater.* **2007**, *19*, 6382–6384.
138. Hiraoka, M.; Hasegawa, T.; Yamada, T.; Takahashi, Y.; Horiuchi, S.; Tokura, Y. On-substrate synthesis of molecular conductor films and circuits. *Adv. Mater.* **2007**, *19*, 3248–3251.
139. Haas, S.; Takahashi, Y.; Takimiya, K.; Hasegawa, T. High-performance dinaphtho-thieno-thiophene single crystal field-effect transistors. *Appl. Phys. Lett.* **2009**, *95*, doi:10.1063/1.3183509.

© 2012 by the authors; licensee MDPI, Basel, Switzerland. This article is an open access article distributed under the terms and conditions of the Creative Commons Attribution license (<http://creativecommons.org/licenses/by/3.0/>).